INTERFERENCE EFFECTS DURING BURNING IN AIR FOR TWO STATIONARY n-HEPTANE DROPLETS

Thesis by

James Foster Rex

Lieutenant, United States Navy

In Partial Fulfillment of the Requirements

for the Degree of

Aeronautical Engineer

California Institute of Technology

Pasadena, California

1955

ACKNOWLEDGEMENT

The author wishes to express his appreciation to Dr. S. S. Penner for suggesting this investigation and for his valuable assistance during the reduction of data. The author is indebted also to Mr. D. Weber for help with the experimental work, and to Mr. D. East for performing many of the film measurements.

ABSTRACT

In order to gain some understanding of droplet interference during burning, experiments have been conducted for the determination of the evaporation constant and flame shapes of two closely spaced n-heptane droplets burning in air. Droplets of approximately the same and of different diameters were used at various distances between the droplet centers.

Experimental results on flame shapes and evaporation constants for closely spaced droplets show somewhat surprising behavior. Thus the apparent flame shape changes very little during the burning of the droplet. The square of the droplet diameter decreases linearly with time for fixed spacing between droplet centers, at least within the experimental limits of accuracy. Since geometrically different conditions are produced continuously during burning, the observed independence of the slope of plots for the square of droplet diameter vs time is not obviously expected. Furthermore, for droplets of different average initial diameters $\overline{D}^o$, the frequency, $\overline{K}'' = \overline{K}'/(\overline{D}^o)^2$, where $\overline{K}'$ is the usual evaporation constant, is well represented as a universal function of the initial spacing between droplet centers $(C^o + \overline{D}^o)$ or adjacent droplet surfaces (C^o).

The evaporation constant $\overline{K}'$ for constant $\overline{D}^o$, and the frequency $\overline{K}''$ for arbitrary values of $\overline{D}^o$, increase at first as C^o is reduced and then decrease again. For large values of C^o, $\overline{K}'$ approaches the numerical value measured in studies on the burning of single droplets. This behavior can be understood in terms of a competition between heat losses to the outside from the flame front surrounding a single droplet, which decrease as the droplets are brought together, and oxygen-deficient atmospheres, which are more likely to occur for very small values of C^o.

Although an acceptable empirical correlation of experimental measurements has been obtained, the processes which determine interference during droplet burning are as yet not understood. In view of the possible practical importance of interference during burning in sprays, additional laboratory studies on the burning of simple geometric arrays, other than two droplets, appear to be indicated.

TABLE OF CONTENTS

PART		PAGE
	Acknowledgement	i
	Abstract	ii
	Table of Contents	iii
	List of Figures	iv
	Nomenclature	vi
I	INTRODUCTION	1
II	EXPERIMENTAL STUDIES ON THE BURNING OF TWO STATIONARY n-HEPTANE DROPLETS	4
	A. Apparatus	4
	B. Experimental Results Relating to Flame Shape and Burning Rate	6
III	EVAPORATION CONSTANTS AND EVAPORATION FREQUENCIES FOR TWO STATIONARY n-HEPTANE DROPLETS BURNING IN CLOSE PROXIMITY	8
	A. Evaporation Constants	8
	B. Evaporation Frequencies	10
IV	FLAME SHAPES	11
	A. Flame Shapes for Single Stationary Fuel Droplets Burning in Air	11
	B. Flame Shapes for Two n-Heptane Droplets Burning in Close Proximity	14
V	CONCLUSIONS	15
	References	16
	Figures	17

LIST OF FIGURES

FIGURE		PAGE
1	Schematic arrangement of flame interference experiment with two droplets burning in close proximity	17
2	Photograph of two n-heptane droplets burning in air	18
3	Schematic diagram of droplet ignition	19
4-28	Experimental results for two n-heptane droplets burning in still air	20-45
(4)	D_1^o = .194 cm, D_2^o = .166 cm, C^o = .020 cm	20
(5)	D_1^o = .181 cm, D_2^o = .174 cm, C^o = .114 cm	21
(6)	D_1^o = .166 cm, D_2^o = .154 cm, C^o = .183 cm	22
(7)	D_1^o = .192 cm, D_2^o = .176 cm, C^o = .230 cm	23
(8)	D_1^o = .165 cm, D_2^o = .142 cm, C^o = .264 cm	24
(9)	D_1^o = .182 cm, D_2^o = .173 cm, C^o = .752 cm	25
	D_1^o = .182 cm, D_2^o = .182 cm, C^o = .892 cm	
(10)	D_1^o = .173 cm, D_2^o = .173 cm, C^o = 1.125 cm	26
	D_1^o = .182 cm, D_2^o = .156 cm, C^o = 1.47 cm	
(11)	D_1^o = .130 cm, D_2^o = .127 cm, C^o = .222 cm	27
	D_1^o = .138 cm, D_2^o = .134 cm, C^o = .208 cm	
(12)	D_1^o = .135 cm, D_2^o = .117 cm, C^o = .313 cm	28
	D_1^o = .124 cm, D_2^o = .124 cm, C^o = .235 cm	
(13)	D_1^o = .133 cm, D_2^o = .122 cm, C^o = .540 cm	29
	D_1^o = .126 cm, D_2^o = .126 cm, C^o = .40 cm	
(14)	D_1^o = .136 cm, D_2^o = .120 cm, C^o = .496 cm	30
	D_1^o = .121 cm, D_2^o = .118 cm, C^o = .384 cm	
(15)	D_1^o = .143 cm, D_2^o = .142 cm, C^o = .533 cm	31
(16)	D_1^o = .141 cm, D_2^o = .135 cm C^o = .538 cm	32

FIGURE		PAGE
(16)	D_1^o = .155 cm, D_2^o = .142 cm, C^o = .496 cm	33
(17)	D_1^o = .156 cm, D_2^o = .147 cm, C^o = .813 cm	34
	D_1^o = .156 cm, D_2^o = .141 cm, C^o = .883 cm	
	D_1^o = .156 cm, D_2^o = .156 cm, C^o = 1.10 cm	
(18)	D_1^o = .208 cm, D_2^o = .155 cm, C^o = .126 cm	35
(19)	D_1^o = .209 cm, D_2^o = .170 cm, C^o = .352 cm	36
(20)	D_1^o = .198 cm, D_2^o = .140 cm, C^o = .375 cm	37
(21)	D_1^o = .167 cm, D_2^o = .115 cm, C^o = .520 cm	38
(22)	D_1^o = .160 cm, D_2^o = .131 cm, C^o = .532 cm	39
(23)	D_1^o = .192 cm, D_2^o = .148 cm, C^o = .026 cm	40
(24)	D_1^o = .208 cm, D_2^o = .164 cm, C^o = .150 cm	41
(25)	D_1^o = .191 cm, D_2^o = .178 cm, C^o = .246 cm	42
(26)	D_1^o = .192 cm, D_2^o = .180 cm, C^o = .355 cm	43
(27)	D_1^o = .202 cm, D_2^o = .179 cm, C^o = .362 cm	44
(28)	D_1^o = .200 cm, D_2^o = .156 cm, C^o = .466 cm	45
29	Variation of the average evaporation constant $\overline{K}'$ with C^o for droplet pairs with different initial average diameters $\overline{D}^o$	46
30	Dependence of the evaporation frequency $\overline{K}''$ on C^o	47
31	Dependence of the evaporation frequency $\overline{K}''$ on $C^o + \overline{D}^o$	48
32	Dependence of the evaporation frequency $\overline{K}''$ on $C^o / \overline{D}^o$	49
33	Schematic diagram of burning fuel droplet	50
34	Plot of experimental and calculated values for C_t vs time, where $C_t = C^o + \overline{D}^o \left[1 - \sqrt{\overline{K}'' t}\right]$	51

NOMENCLATURE

a	vertical distance from center of droplet to lower flame surface
b	horizontal distance from center of droplet to outside flame surface
C^o	initial minimum distance between adjacent droplet surfaces
C	minimum distance between adjacent droplet surfaces at time t
D^o	initial droplet diameter
D	droplet diameter at time t
K'	evaporation constant
K''	evaporation frequency
subscript 1	identifies the larger of two droplets
subscript 2	identifies the smaller of two droplets
$\overline{D}^o$	arithmetic average value of D^o for droplets 1 and 2
$\overline{D}$	arithmetic average value of D for droplets 1 and 2
$\overline{K}'$	arithmetic average value of K' for droplets 1 and 2
$\overline{K}''$	arithmetic average value of K'' for droplets 1 and 2
$\overline{D}'$	size constant in Rosin-Rammler distribution law
n	distribution constant in Rosin-Rammler distribution law
w	weight fraction of the spray composed of droplets with diameter larger than D

I. INTRODUCTION

A considerable number of theoretical and experimental papers have been published on the burning of single droplets of fuel (1-5). Experimental studies have been performed on single droplets suspended from fine quartz fibers and burning in an oxidizing atmosphere (5). A reasonable theoretical prediction of mass burning rate for single droplets can be obtained on the assumption that mass transport by diffusion to the flame surface and heat conduction to the burning droplet control the burning rate (4).

Recently an attempt has been made by Graves and Gerstein at the NACA to utilize the results obtained in single droplet studies for the description of burning rates in sprays (6). These authors started with the results of an important theoretical study carried out some years ago by Probert (7). Probert made the following assumptions:

(a) The spray particle size follows the Rosin-Rammler distribution law,

$$w = e^{-(D/\bar{D}')^n}, \qquad [1]$$

where w equals the volume fraction or weight fraction of the spray composed of drops with diameters greater than D, $\bar{D}'$ is called the size constant, and n is usually referred to as the distribution constant.

(b) The rate of burning of the droplets is taken to be proportional to the first power of the droplet diameter. In this case it is easily shown that

$$D^2 = (D^o)^2 - K't \qquad [2]$$

where D is the droplet diameter at any time, D^o is the initial diameter, and K'

(which has the dimensions of area per unit time), is known as the evaporation constant.

Probert has shown how to compute the percentage of unburned fuel as a function of $\sqrt{K' t_r} / \bar{D}'$ for values of n between 2 and 4, where t_r is the residence time of the burning droplets. Recently correlations similar to those of Probert have been worked out for droplet distribution laws other than the Rosin-Rammler distribution law (8).

Equation [2], which relates droplet diameter to the burning time, is known to correlate all of the observed results for the steady burning of single fuel droplets in an oxidizing atmosphere (4). Therefore, it is of obvious interest to determine whether or not the value of the evaporation constant, K', for single droplet theory or experiment has any relation to the value of K' appropriate for spray combustion. Graves and Gerstein attempted to answer this question by measuring the combustion efficiency as a function of oxygen concentration for a single tubular combustor using iso-octane as fuel and countercurrent injection. They compared observed combustion efficiencies with calculated combustion efficiencies using Probert's theoretical analysis in conjunction with values of K' measured for the burning of single droplets. This comparison showed that all of the observed results could not be explained unless spray combustion involves effects, at least for oxygen concentrations below 24 percent, which can be ignored in the burning of single droplets. In connection with the use of single droplet data for studies on spray combustion, it is therefore, of obvious

importance to carry out laboratory studies on interference between droplets during burning.

Although, as a general rule, statistical arrays are more easily interpreted than small numbers of droplets, such as 2, 4, etc., experimental studies on small numbers of droplets may provide a clue for the important physico-chemical processes operative in droplet interference during burning. For this reason experiments have been carried out on the variation of K' with droplet size and droplet spacing for two closely spaced droplets.

II. EXPERIMENTAL STUDIES ON THE BURNING OF TWO STATIONARY n-HEPTANE DROPLETS

A. Apparatus

In order to record the flame shape and the decrease in droplet diameter with time, the droplets were suspended on thin quartz fibers which were secured by means of a Sauereisen cement to a metal rod. The rod was bent at an angle of 90 degrees at one end to insure a large supporting surface. The rod was supported on a stand by means of a clamp. Rods of various diameters were used for different minimum spacings between the adjacent surfaces of the droplets, C^{o} (see Fig. 1). The fibers were enclosed in a circular plastic tube of several inches diameter in order to eliminate ambient air currents. Single droplets of fuel were suspended from the fibers by forcing fuel through a hypodermic needle onto the fiber. The droplet diameters varied from .117 to .209 cms. The droplets were reasonably spherical as shown in the photograph of Fig. 2.

The drops were ignited by using an automobile ignition system connected to electrodes which straddled the two quartz fibers through holes in the tube (see Fig. 3). This method of ignition was found to be useful for values of C^{o} less than or equal to 0.8 cms. For runs of C^{o} greater than 0.8 cms, a match was used in order to ignite the droplets.

An electrically driven Arriflex 35mm movie camera was used for photographing the burning droplets. In order to photograph the flame front, a 100 watt bulb was placed behind and off to one side of the burning drops. This method silhouetted the drops and also left the flame front visible as shown in Fig. 2. A ten inch adapter tube and

telephoto lens were employed in order to obtain as large an image as possible on each frame of film. Kodak Plus X and Kodak Super XX films were used with apertures of f6 and f9, respectively.

A stroboscope served as timing standard. A ten inch circular aluminum plate, with three holes placed 120 degrees apart, was secured to a 75 RPM constant speed motor giving 3.75 flashes per second. The stroboscope was placed directly behind the burning drops. The camera speed was adjusted to almost 25 frames per second, as determined from observations of the stroboscope.

A 3/32 inch ball bearing was photographed at the beginning of each 100 foot roll of film used. The image served for calibration and was obtained under the same focusing conditions as for the burning droplets.

The film was measured by using a microfilm recorder and a steel scale graduated in millimeters. Two measurements were made on each drop per frame, namely, the two perpendicular diameters inclined 45 degrees to the major and minor axes in the plane of observation. The mean value of these two readings was recorded as the "effective diameter" of the droplet. It is easily shown that if the major and minor axes do not differ greatly, as was the case in our experiments, then the volume of a sphere with the measured effective diameter is not greatly different from that of the prolate spheroid, which actually corresponds to the shape of our droplets. In most cases measurements were taken from ignition to burn out and recorded approximately every fifth or sixth frame. The flame shape parameters a_1, a_2, b_1, and b_2 (see Fig. 1), were also measured.

B. Experimental Results Relating to Flame Shape and Burning Rate

Experimental studies were carried out for two stationary n-heptane droplets in air and showed that the square of the droplet diameter, D^2, was a linear function of the time, t, for each of the burning droplets, at least within the limits of experimental accuracy. The flame shape parameters were found to vary remarkably little as the droplets burned. In Figs. 4 to 28 and in Table I are summarized all of the observed experimental results. The flame shape parameters are plotted as functions of time for those sets of data for which they were measured. The squares of the droplet diameters, D_1^2 and D_2^2, are plotted as a function of the time for all of the measurements. "Best" straight lines have been drawn through the experimentally determined points except for those cases in which the data were not adequately represented by linear correlations. In some cases the measured data suggest periodic variations of observed parameters (see, particularly, Figs. 23 to 28). Data of D^2 as a function of t, which could not be correlated by straight lines, have been ignored in subsequent attempts at finding universal correlations.

In several instances, where droplets of greatly different sizes were used, observations were possible on the larger remaining droplet after the smaller droplet had burned out. In most of these cases the slope of the D^2 vs t curve changed rather abruptly and yielded data in fair agreement with the known single droplet results ($K' \simeq 0.008$ cm^2/sec) after the smaller droplet had burned completely (see Figs. 18 to 22). For droplets of nearly equal diameters ($D_1^o \simeq D_2^o$) the evaporation constants K_1' and K_2' are nearly equal (see Figs. 4 to 17).

TABLE I EXPERIMENTAL RESULTS FOR TWO n-HEPTANE DROPLETS BURNING IN STILL AIR

FIGURE	D_1^o, cm	D_2^o, cm	C^o, cm	K_1'	K_2'
4	0.194	0.166	0.020	0.0094	0.0082
5	0.181	0.174	0.114	0.0096	0.0094
6	0.166	0.154	0.183	0.0135	0.0130
7	0.192	0.176	0.230	0.0105	0.0096
8	0.165	0.142	0.264	0.0136	0.0122
9	0.182	0.173	0.752	0.0153	0.0141
9	0.182	0.182	0.892	0.0140	0.0140
10	0.173	0.173	1.125	0.0139	0.0133
10	0.182	0.156	1.47	0.0124	0.0115
11	0.130	0.127	0.222	0.0080	0.0072
11	0.138	0.134	0.208	0.0068	0.0063
12	0.135	0.117	0.313	0.0085	0.0085
12	0.124	0.124	0.235	0.0070	0.0070
13	0.133	0.122	0.540	0.0091	0.0090
13	0.126	0.126	0.40	0.0086	0.0086
14	0.136	0.120	0.496	0.0091	0.0068
14	0.121	0.118	0.384	0.0074	0.0074
15	0.143	0.142	0.533	0.0118	0.0110
16	0.141	0.135	0.538	0.0097	0.0093
16	0.155	0.142	0.496	0.0122	0.0114
17	0.156	0.147	0.813	0.0123	0.0113
17	0.156	0.141	0.883	0.0110	0.0112
17	0.156	0.156	1.10	0.0107	0.0108
18	0.208	0.155	0.126	0.0107	0.0104
19	0.209	0.170	0.352	0.0123	0.0109
20	0.198	0.140	0.375	0.0090	0.0089
21	0.167	0.115	0.520	0.0150	0.0090
22	0.160	0.131	0.532	0.0140	0.0150
23	0.192	0.148	0.026	-	0.0068
24	0.208	0.164	0.150	-	0.0124
25	0.191	0.178	0.246	0.0157	-
26	0.192	0.180	0.355	-	-
27	0.202	0.179	0.362	-	-
28	0.200	0.156	0.466	0.0133	-

III. EVAPORATION CONSTANTS AND EVAPORATION FREQUENCIES FOR TWO STATIONARY n-HEPTANE DROPLETS BURNING IN CLOSE PROXIMITY

A. Evaporation Constants

If the evaporation constant, K', of a stationary fuel droplet suspended from a quartz fiber is modified extensively by the presence of a second droplet burning in close proximity, then one would expect the value of K' to depend both on the instantaneous values of the droplet diameters and on the distance between the droplets. In other words, one might expect K' to be a function of the time. Contrary to this idea, it has been found that K' is constant, within the experimental limits of accuracy, for two droplets of n-heptane burning in close proximity. In fact, as will be shown in greater detail presently, the observed values of K' seem to depend only on the initial droplet diameters and on the initial spacing between the droplets burning in air.

The observed values of $\overline{K}' = (1/2)\ (K_1' + K_2')$ for droplets in which D_1^o and D_2^o did not differ by more than 20% are plotted as a function of C^o in Fig. 29. Reference to Fig. 29 shows that the experimental results fall roughly into two categories depending on the initial average droplet diameter $\overline{D}^o = (1/2)\ (D_1^o + D_2^o)$. The numbers in Fig. 29 correspond to the numbers of the figures in which the raw data of D_1^2 vs t and of D_2^2 vs t are shown (Figs. 4 to 17). Reference to Fig. 29 shows that the average evaporation constant increases when C^o is reduced from larger values with negligible droplet interference, presumably because heat losses from the flame surface are reduced by the proximity of a second heat source for sufficiently small values of C^o; $\overline{K}'$ reaches a maximum and then decreases again

as C^o is made still smaller. A decrease in $\overline{K}'$ for very small values of C^o could be produced through the creation of oxygen-deficient atmospheres resulting from increased competition for the oxygen supply furnished by convection and diffusion. On the basis of the proposed picture the maximum in plots of $\overline{K}'$ vs C^o results through a balance between two opposing factors, viz., decreased heat loss and decreased oxygen supply. The proposed interpretation, if applicable to spray combustion, may be of considerable practical importance.

A number of attempts were made to relate $\overline{K}'$ with simple functions of C^o, $C^o/\overline{D}^o$, $C^o + \overline{D}^o$, $(C^o + \overline{D}^o)/\overline{D}^o$, etc., in order to reduce the scatter of experimental points for different values of $\overline{D}^o$. These efforts were, however, unsuccessful and suggest that the evaporation constant, K', which is independent of initial droplet diameter in single droplet studies, loses its significance as a basic correlating parameter for two droplets burning in close proximity. Whether or not this conclusion applies to sprays cannot be said without further experimental work. In the meantime, however, it appears that, without further proof, applicability of the droplet burning relation $D^2 = (D^o)^2 - K't$, used in Probert's analysis, is subject to some question. The fact that $\overline{K}'$ varies with $\overline{D}^o$ is shown more directly by plotting $\overline{K}'$ as a function of $\overline{D}^o$ for a group of experimental data with nearly equal values of C^o.

Two burning droplets meet the requirements of geometric similarity when they have the same values of $C/\overline{D}$ and of $\overline{D}$. It

is easily shown from plots of $C/\bar{D}$ vs $\bar{D}$ that (nearly) intersecting curves are characterized by greatly different values of $\bar{K}'$ if the values of $\bar{D}^o$ are different. In other words, the value of the evaporation constant is determined primarily by the initial conditions and, if at all, only to a lesser extent by geometrical arrangement. It is possible that the initial convection currents, which depend on the initial conditions, exert a profound influence on the burning of two adjacent droplets throughout the droplet life.

B. Evaporation Frequencies

In view of the apparent dependence of $\bar{K}'$ on $\bar{D}^o$, attempts were made to find a simple function of $\bar{K}'$ and $\bar{D}^o$ which would depend only on C^o or on a known function of C^o and $\bar{D}^o$. An obvious choice is the ratio $\bar{K}'' = \bar{K}'/(\bar{D}^o)^2$ to which we shall refer as the evaporation frequency.

In Figs. 30 to 32 we have plotted $\bar{K}''$ as a function of C^o, $C^o + \bar{D}^o$, and $C^o/\bar{D}^o$, respectively. Reference to Figs. 30 to 32 shows that a fair correlation of all of the experimental data has been obtained, the scatter being perhaps smaller in the plots using C^o and $C^o + \bar{D}^o$ as abscissa than in the plot using the dimensionless quantity $C^o/\bar{D}^o$. In the absence of an adequate theory concerning droplet interference, the significance of the observed "correlations" is obscure, as is also any extrapolation to sprays. For this reason we must content ourselves with the observation that, for two n-heptane droplets burning in close proximity, the observed values of $\bar{K}'/(\bar{D}^o)^2$

are fairly well represented as a function of either C^o or of $C^o + \overline{D}^o$. Constancy of the evaporation frequency, except for variations in C^o, means that the fundamental burning rate law for fixed values of C^o has the form

$$(\overline{D})^2 = (\overline{D}^o)^2 - \overline{K}'' (\overline{D}^o)^2 \quad t \qquad [3]$$

IV. FLAME SHAPES

The flame shapes for two droplets, as for single droplets, are determined largely by convection currents. A qualitative description of flame shapes can be given on the basis of available experimental measurements.

A. Flame Shapes for Single Stationary Fuel Droplets Burning in Air

According to an elaboration* of observations by Kumagai and Kimura (9), a realistic description can be obtained for the flame shape surrounding a burning single, stationary, droplet of fuel in air by allowing for the influence of free convection.

A burning fuel droplet in air must produce free convection currents. In Fig. 33 we show a schematic diagram of the flame shape for a single droplet. We shall assume that the convection velocity corresponds to a uniform flow with velocity U at some distance upstream from the initial undisturbed flame front. The combination of burning droplet and convective flow then acts as a source in a uniform flow field and, at steady burning, establishes the flow pattern corresponding to a half body as lower boundary. The stream surface through the

---

*The present discussion is based on ideas formulated by L. Lees and S. S. Penner.

lower stagnation point may be thought of as dividing initially the stream lines originating from the source (fuel droplet) and the streamlines established by convective flow. This situation is, however, unstable and diffusive transport of oxidizer and fuel across the stream surface must be established. The tangential flow velocities at the stream surface of fuel vapor and air are initially equal. Presumably concentration and temperature gradients are established during steady burning in such a way that diffusive transport of fuel and oxygen brings a stoichiometric mixture roughly to the stream surface, thereby making the lower stream surface a flame surface.

Most of the fuel vapor is deflected around the stream surface and ultimately moves vertically upward through a cylinder of diameter b. An air flow is established parallel to the fuel flow, moving with the same uniform velocity U as the approach stream and the fuel vapor. Hence conditions are established for the formation of an overventilated diffusion flame and the flame height h can presumably be calculated, in first approximation, from the classical treatment of Burke and Schumann for diffusion flames.

The preceding remarks may be summarized by noting that the effect of free convection is, in first approximation, a distortion of the spherical flame front to a flame surface whose lower boundary is the stream surface corresponding to a source of strength $\dot{m}_F/\rho_F$ ($\dot{m}_F$ = mass rate of burning of fuel droplet, ρ_F = density of fuel vapor)

in a uniform flow of velocity U; the upper flame surface may be described as the flame front for a cylindrical diffusion flame with the inside cylinder of diameter b and the flow velocities of fuel and air equal to U.

The postulated description of the flame surface leads to results which are in accord with the observations of Kumagai and Kimura. Thus

$$2\,b = \sqrt{2\,\dot{m}_F / \rho_F \pi\, U} \quad , \qquad [4]$$

and

$$2b/a = 2\sqrt{2}. \qquad [5]$$

Furthermore, since $U \sin\theta$ (i.e., the tangential flow velocity of air at the stream surface) must be equal to the tangential flow velocity of fuel vapor, one would expect that U and $\dot{m}_F$ are proportional to each other.

Thus

$$U \sim D \qquad [6]$$

since $\dot{m}_F$ is known to be proportional to the diameter of the burning fuel droplet. Also b should be a constant for a given fuel droplet and oxidizing medium; Kumagai and Kimura (9) found b to remain unchanged, for example, for cetane oil as the droplet diameter was increased from about 0.07 to 0.12 cm.

The functional form of the relation between $\underline{b}$, $\dot{m}_F$, and U, as given in Equation [4], is in accord both with the picture of a lower flame surface corresponding to the stream surface and also with the following considerations. Most of the energy transport to the fuel droplet occurs from the upper flame surface. The area of this surface (for $h \geq b$) is roughly proportional to bh. But for a cylindrical diffusion flame $h \sim b^2 U$. Hence the flame surface varies as $b^3 U$. The energy transport to the fuel droplet is proportional to the product of flame surface and temperature gradient at the flame surface. The latter quantity would be expected to vary roughly as $1/b$. Finally, the total energy transport to the fuel droplet must be proportional to $\dot{m}_F / \rho_F$. Therefore,

$$b^2 U \sim \dot{m}_F / \rho_F$$

or

$$b \sim \sqrt{\dot{m}_F / \rho_F U} \ .$$

Although the picture of the formation of a heterogeneous diffusion flame given above seems qualitatively correct, it is apparent that a complete solution of the problem under consideration cannot be obtained without a quantitative analysis of energy transport to the droplet from the flame boundaries. However, the qualitative considerations based on the work of Kumagai and Kimura and sketched above suggest that the following important results will be obtained: (a) $\dot{m}_F$ weakly dependent on flame shape; (b) U and $\underline{h}$ proportional to D; (c) $\underline{h}$ proportional to b^2; (d) $\underline{b}$ independent of D.

B. Flame Shapes for Two n-Heptane Droplets Burning in Close Proximity

For two n-heptane droplets burning in close proximity it has

already been noted that a_1, b_1, a_2, and b_2 change very little during droplet burning. Furthermore, reference to Figs. 4 to 8, Fig. 15 and Figs. 18 to 28 shows that the ratio of $\underline{b}$ to $\underline{a}$ is not sensibly different from unity and does not seem to depend strongly on C^o. In some cases, the distances of the flame surfaces from the droplet surfaces remained constant during burning (see Fig. 2).

The droplet spacing parameter C is, of course, determined through the geometric arrangement. Thus

$$C = C^o + (1/2)(D_1^o - D_1) + (1/2)(D_2^o - D_2)$$

or

$$C = C^o + (1/2)D_1^o \left[1 - \sqrt{K_1' t / (D_1^o)^2}\right] + (1/2)D_2^o \left[1 - \sqrt{K_2' t / (D_2^o)^2}\right]. \quad [7]$$

Needless to say, the time dependence of C is well represented by Equation [7], as shown in Fig. 34.

V. CONCLUSIONS

The investigations of droplet interference during burning described in this report have shown a number of unexpected results which may well be of importance for a fundamental understanding of spray combustion. In particular, the fact that the evaporation constant is no longer independent of droplet diameter for fixed spacing requires further study. An obvious extension of the present experimental program leads to burning rate studies on simple geometric arrays, such as five droplets. It is also apparent that some fundamental theoretical studies on interference during burning are required.

REFERENCES

1. "The Burning of Single Drops of Fuel: Part I, Temperature Distribution and Heat Transfer in Pre-Flame Region," by G. A. E. Godsave, National Gas Turbine Establishment (England) Report No. R. 66, 1950.

2. "The Burning of Single Drops of Fuel: Part II, Experimental Results," by G. A. E. Godsave, National Gas Turbine Establishment (England) Report No. R. 87, 1951.

3. "An Experimental Study of the Burning of Single Drops of Fuel in Air at Pressures up to Twenty Atmospheres," by A. R. Hall and J. Diederichsen, Fourth (International) Symposium on Combustion, Williams and Wilkins Company, Baltimore, 1953, pp. 837-846.

4. "On the Burning of Single Drops of Fuel in an Oxidizing Atmosphere," by M. Goldsmith and S. S. Penner, Jet Propulsion, Vol. 24, 1954, pp. 245-251. See also Introduction to the Study of Chemical Reactions in Flow Systems, by S. S. Penner, Butterworths Publications, Ltd., London 1955, Chapter 4.

5. "Experiments on the Burning of Single Drops of Fuel in Oxygen-Inert Gas Mixtures," by M. Goldsmith and C. K. Perkins, Technical Report No. 4, Contract No. DA-495-Ord-446, California Institute of Technology, May 1954.

6. "Some Aspects of the Combustion of Liquid Fuels," by C. C. Graves and M. Gerstein in Combustion Researches and Reviews, 1955, Butterworths Publications, Ltd., London 1955.

7. "The Influence of Spray Particle Size and Distribution in the Combustion of Oil Droplets," by R. P. Probert, Philosophical Magazine, Vol. 37, 1953, pp 94-105.

8. "On the Combustion Rate of a Group of Fuel Particles Injected Through a Swirl Nozzle," by Y. Tanasawa, Technology Reports of Tohoku University, Vol. 18, 1954, pp. 195-208, Sendai, Japan.

9. "Combustion of Fuel Droplets," by S. Kumagai and I. Kimura, Science of Machine, Vol. 3, 1951, pp. 431-434.

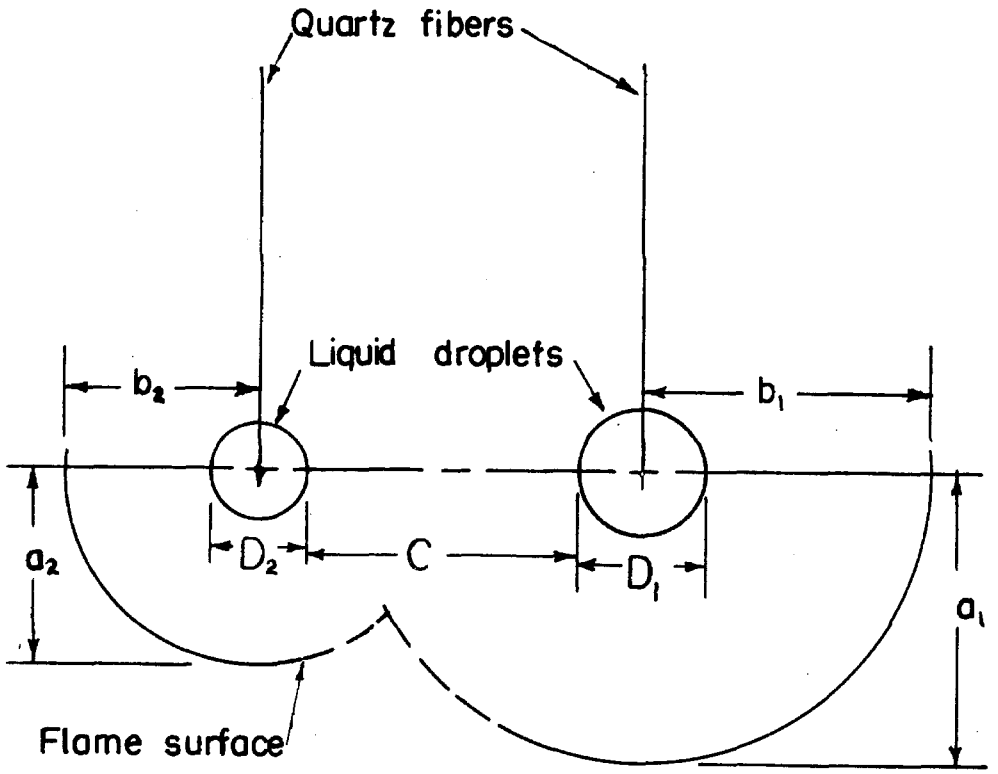

FIGURE I. SCHEMATIC ARRANGEMENT OF FLAME INTERFERENCE EXPERIMENT WITH TWO DROPLETS BURNING IN CLOSE PROXIMITY

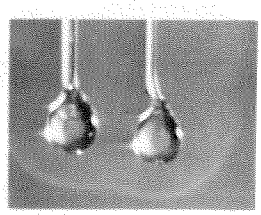

IGNITION

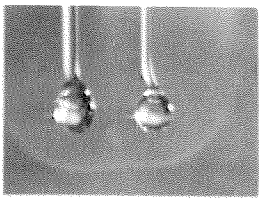

T=1.44 SEC.

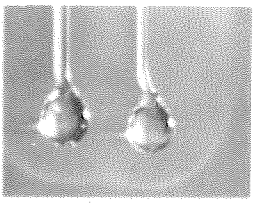

T=0.53 SEC.

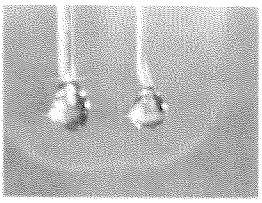

T=1.70 SEC.

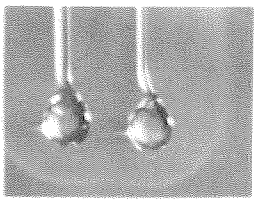

T=0.75 SEC.

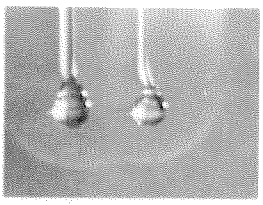

T=1.90 SEC.

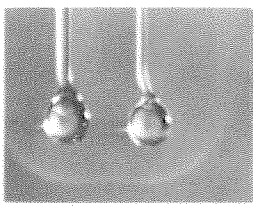

T=0.92 SEC.

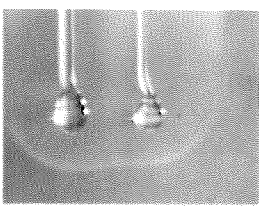

T=2.15 SEC.

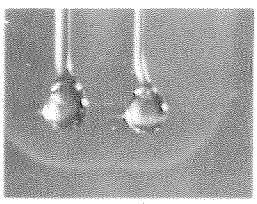

T=1.28 SEC.

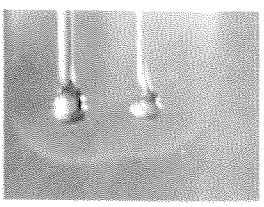

T=2.40 SEC.

FIGURE 2. PHOTOGRAPH OF TWO n-HEPTANE DROPLETS BURNING IN AIR (D_1^o= 0.181cm, D_2^o=0.174cm, C^o=0.114cm)

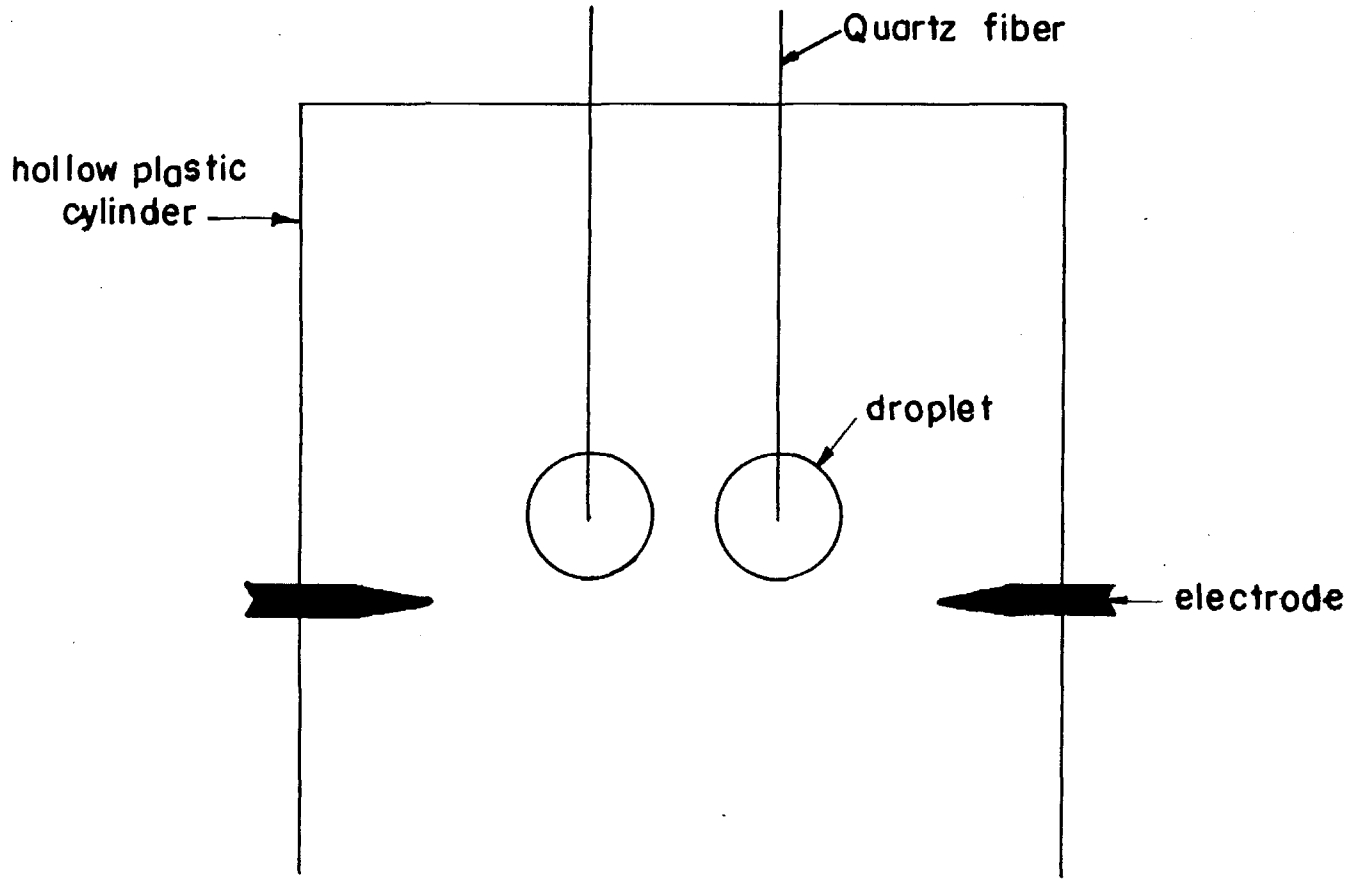

FIGURE 3. SCHEMATIC DIAGRAM OF DROPLET IGNITION

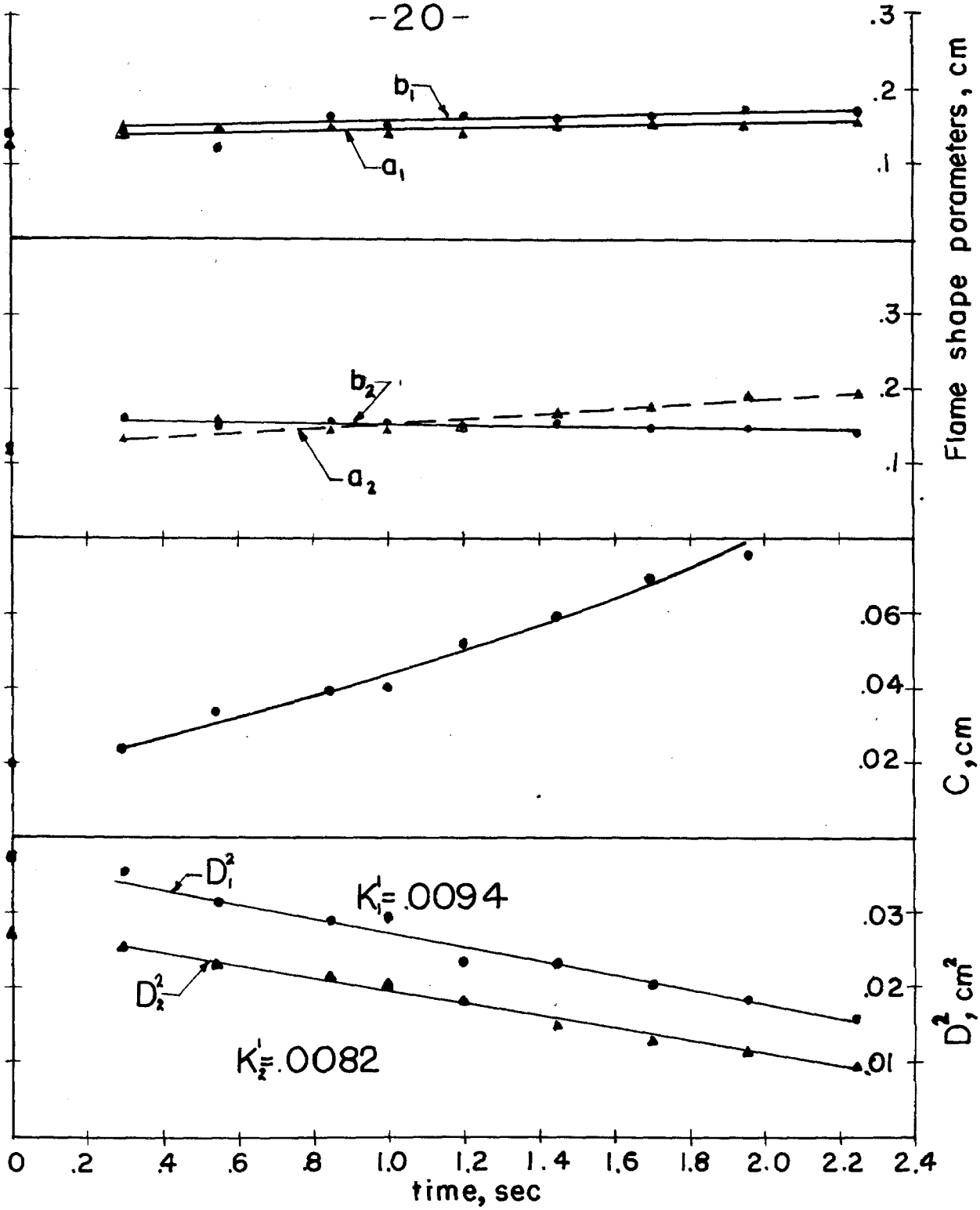

FIGURE 4. EXPERIMENTAL RESULTS FOR TWO n-HEPTANE DROPLETS BURNING IN STILL AIR (D_1^o=0.194 cm, D_2^o=0.166cm, C^o=0.020cm)

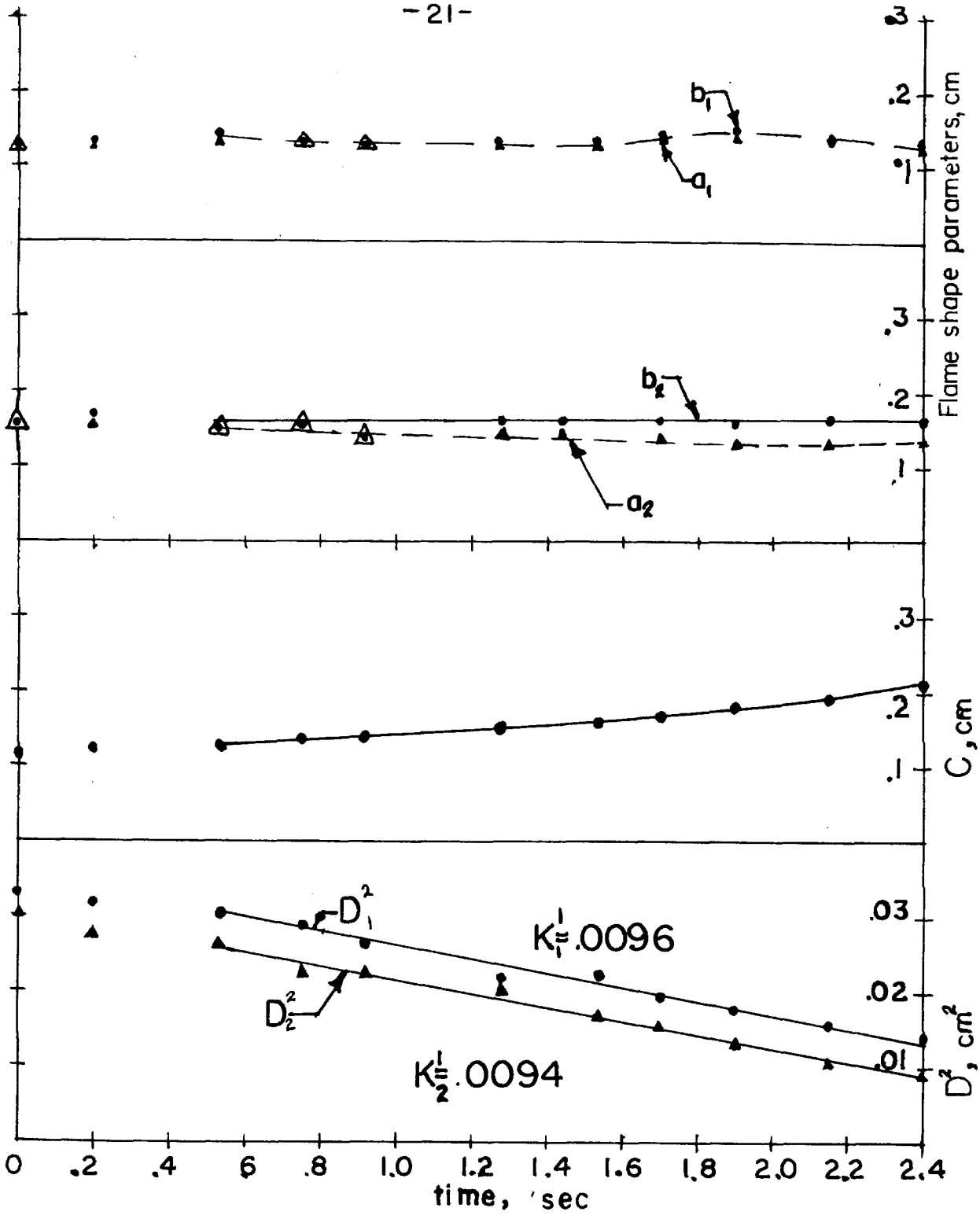

FIGURE 5. EXPERIMENTAL RESULTS FOR TWO n-HEPTANE DROPLETS BURNING IN STILL AIR (D_1^o=0.181cm, D_2^o=0.174cm, C^o=0.114 cm)

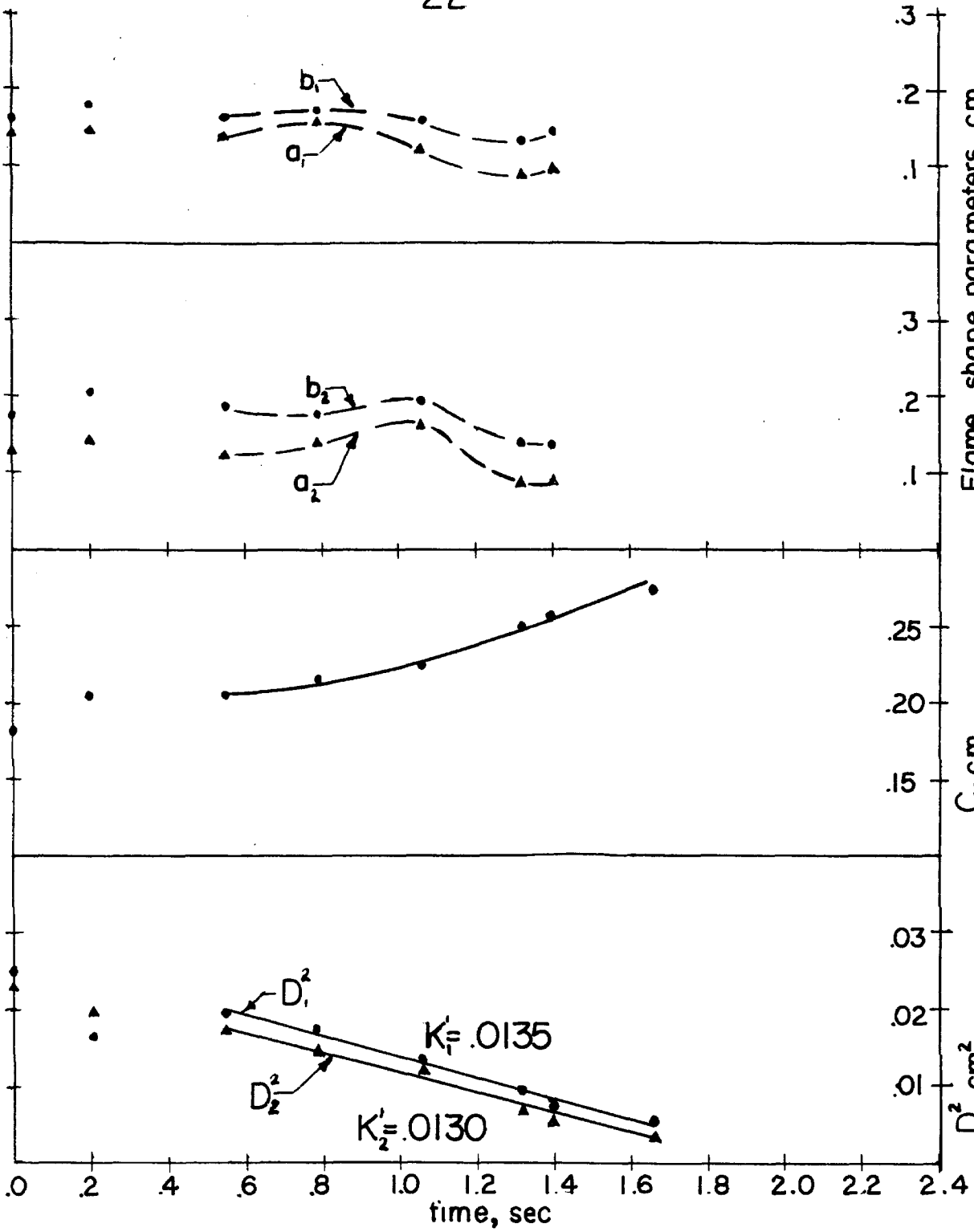

FIGURE 6. EXPERIMENTAL RESULTS FOR TWO n-HEPTANE DROPLETS BURNING IN STILL AIR (D_1^o=0.166 cm, D_2^o=0.154cm, C^o=0.183cm)

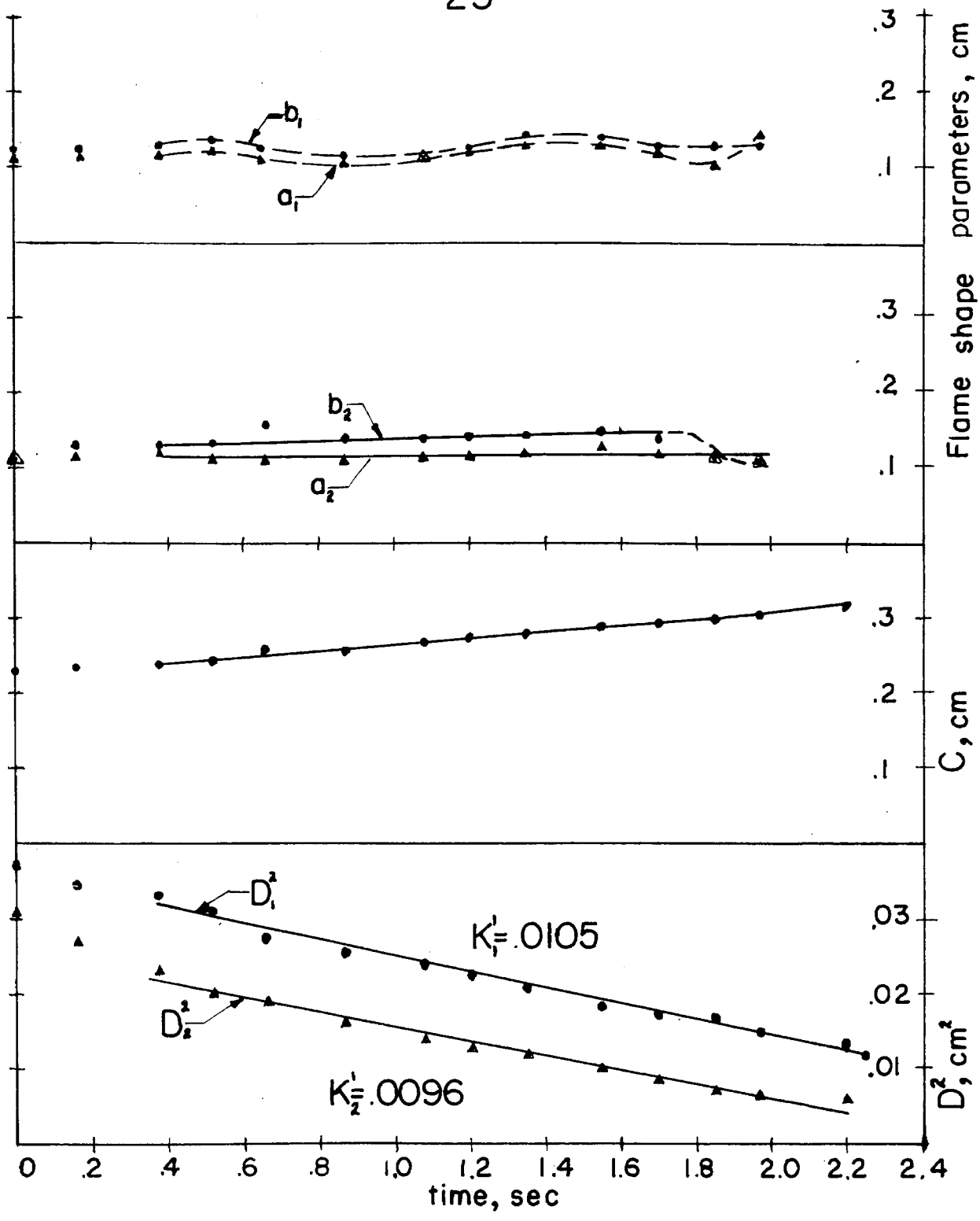

FIGURE 7. EXPERIMENTAL RESULTS FOR TWO n-HEPTANE DROPLETS BURNING IN STILL AIR (D_1^o=0.192 cm, D_2^o=0.176cm, C^o=0.230 cm)

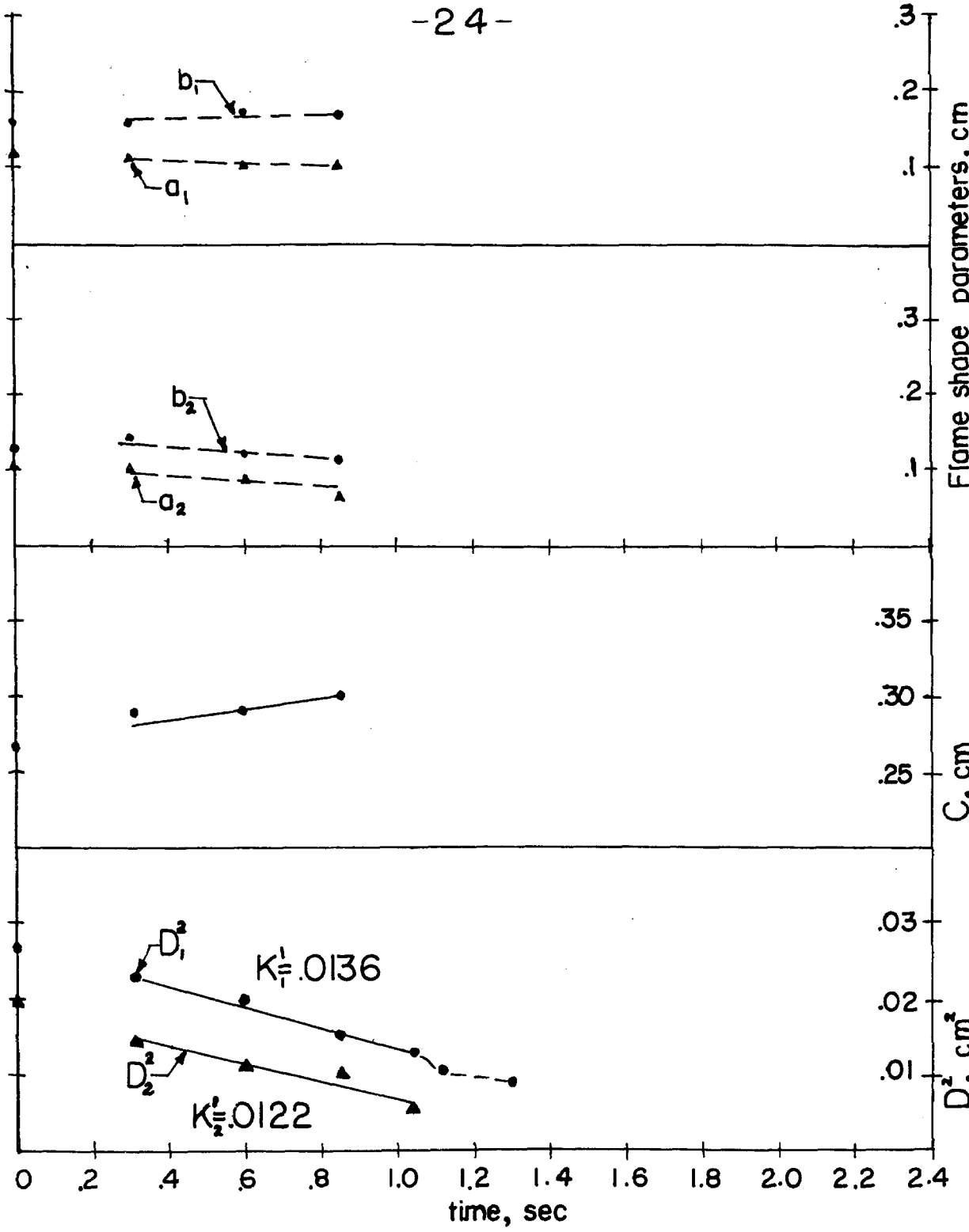

FIGURE 8. EXPERIMENTAL RESULTS FOR TWO n-HEPTANE DROPLETS BURNING IN STILL AIR (D_1^o=0.165 cm, D_2^o=0.142cm, C^o=0.264cm)

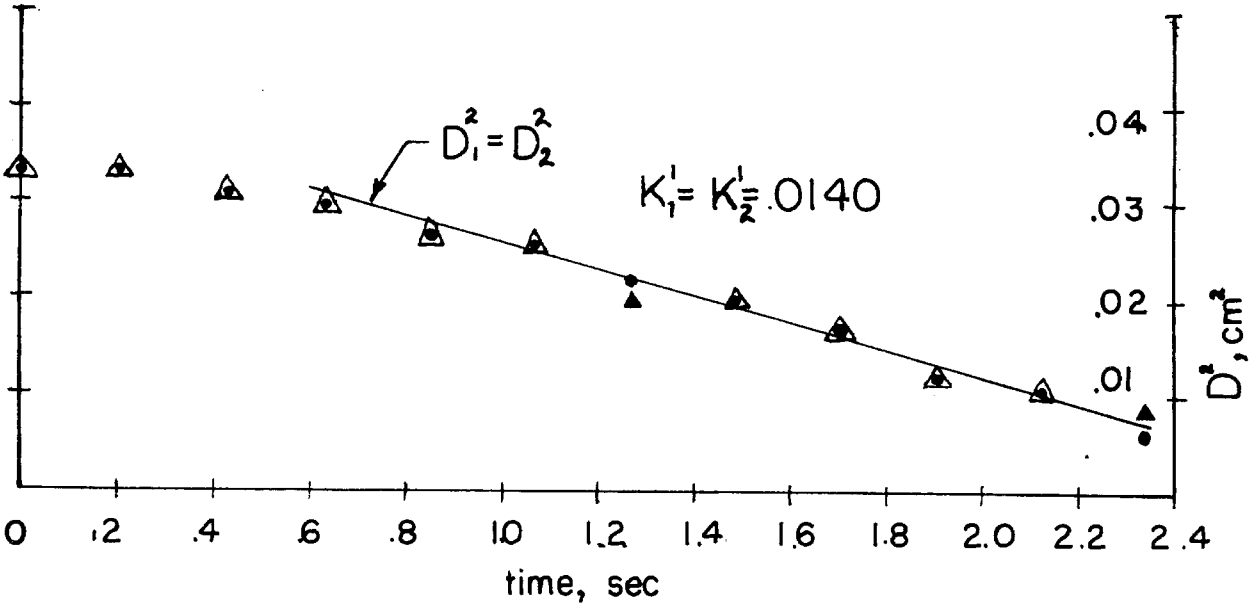

$(D_1^o = 0.182\text{cm},\ D_2^o = 0.182\text{cm},\ C^o = 0.892\text{cm})$

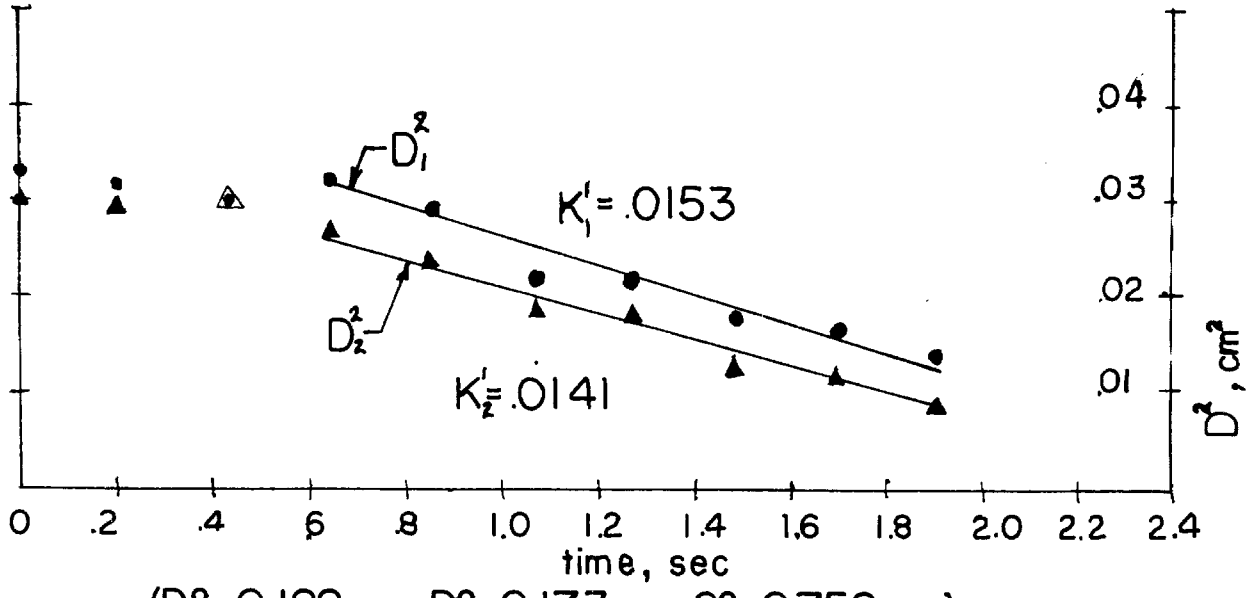

$(D_1^o = 0.182\text{cm},\ D_2^o = 0.173\text{cm},\ C^o = 0.752\text{cm})$

FIGURE 9. PLOTS OF D^2 vs time FOR TWO n-HEPTANE DROPLETS BURNING IN STILL AIR FOR VARIOUS C^o

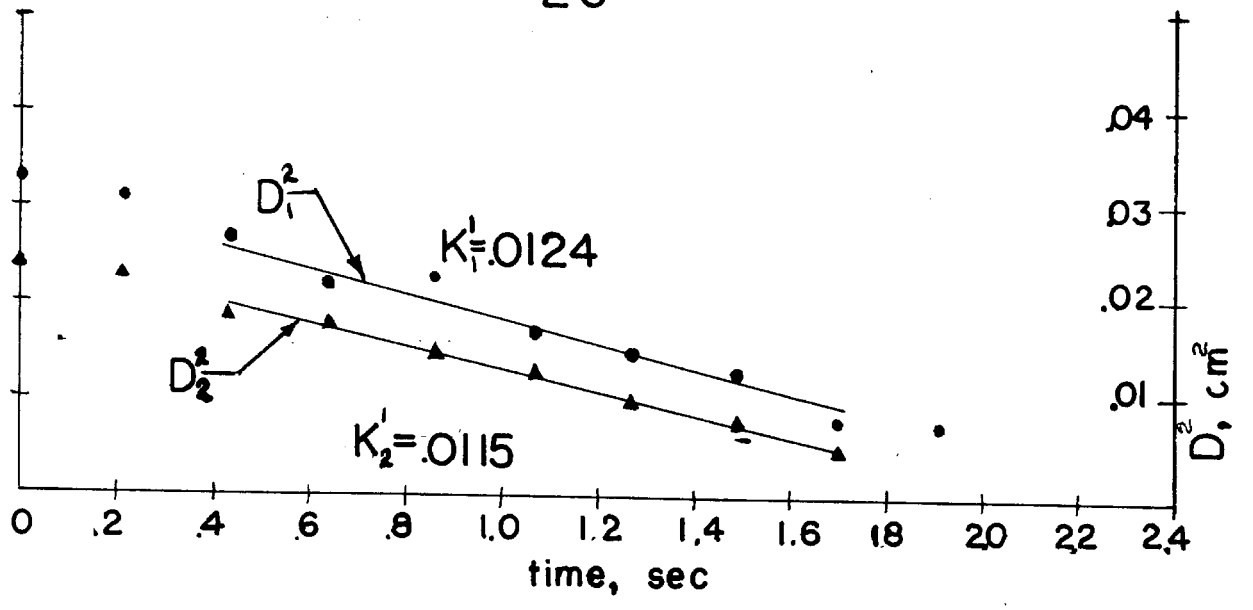

(D^o=0.182cm , D^o=0.156 cm , C^o= 1.47cm)

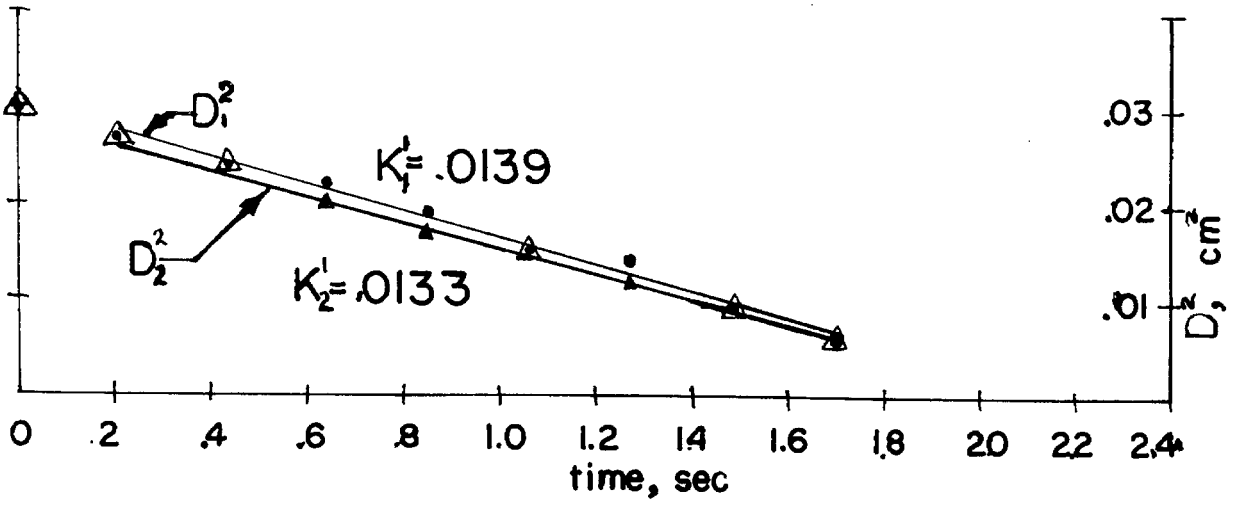

(D_1^o=0.173cm , D_2^o=0.173cm , C^o=1.125 cm)

FIGURE 10. PLOTS OF D^2 vs time FOR TWO n -HEPTANE DROPLETS BURNING IN STILL AIR FOR VARIOUS C^o

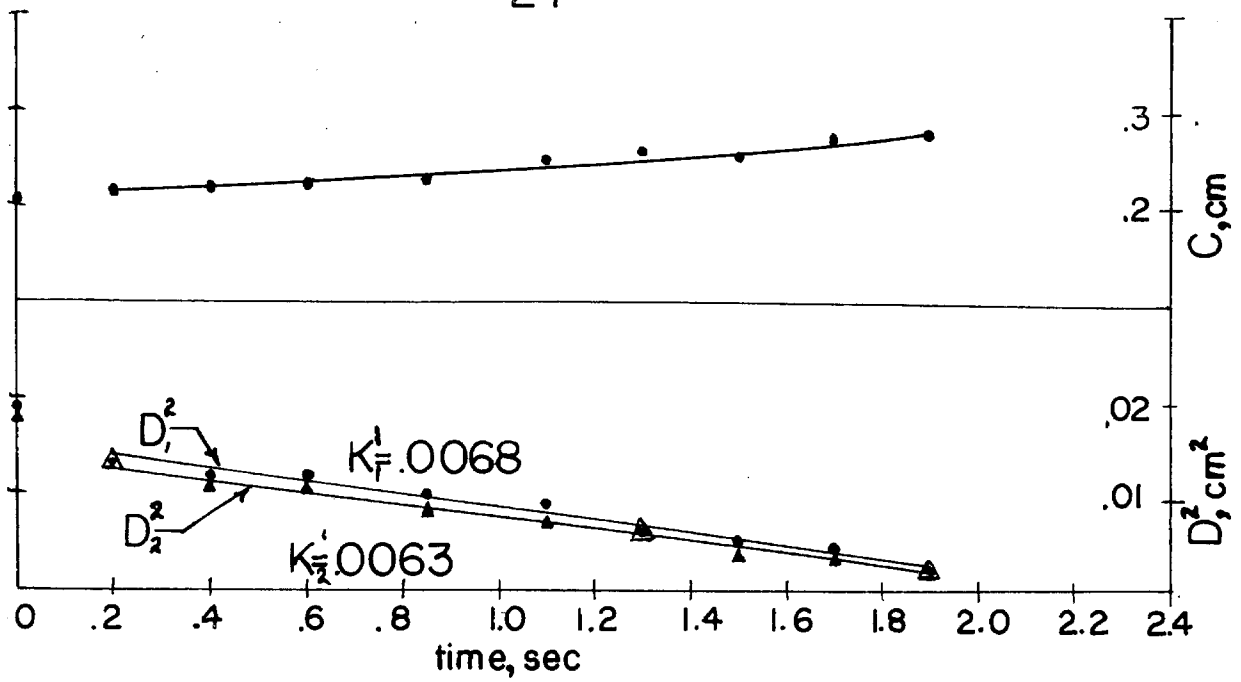

(D_1^o = 0.138cm, D_2^o = 0.134cm, C^o = 0.208cm)

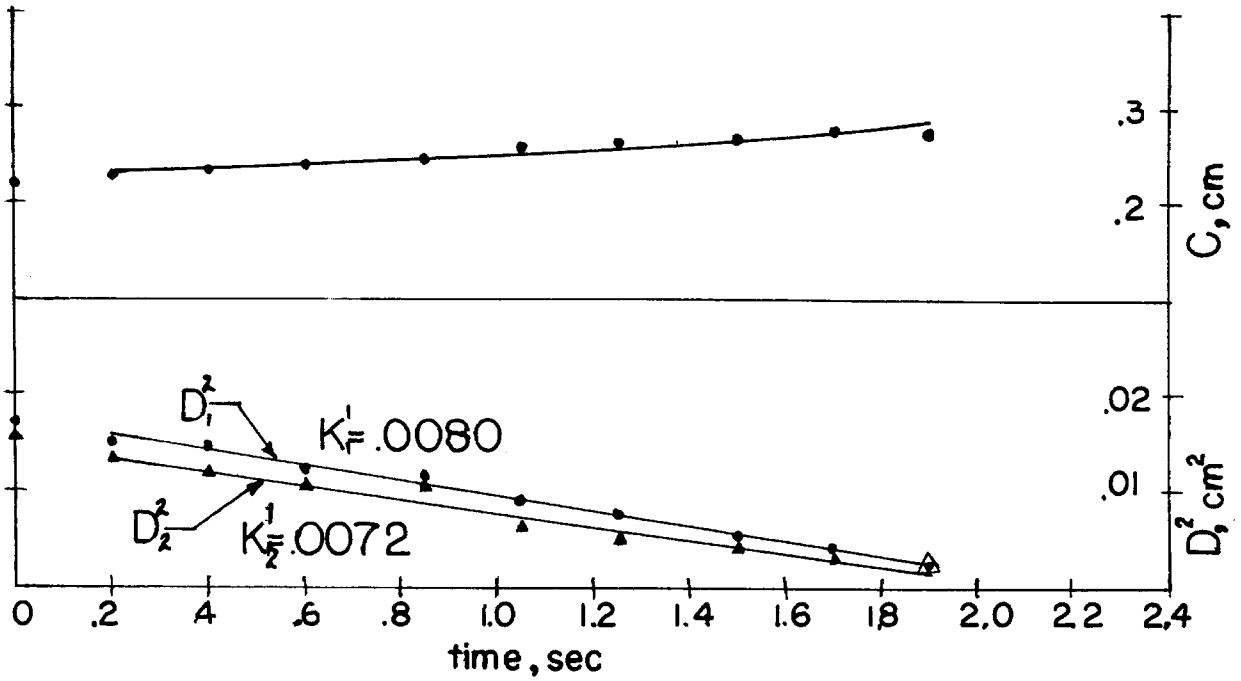

(D_1^o = 0.130cm, D_2^o = 0.127cm, C^o = 0.222cm)

FIGURE 11. PLOTS OF D^2 vs time and C vs time FOR TWO n-HEPTANE DROPLETS BURNING IN STILL AIR FOR VARIOUS C^o

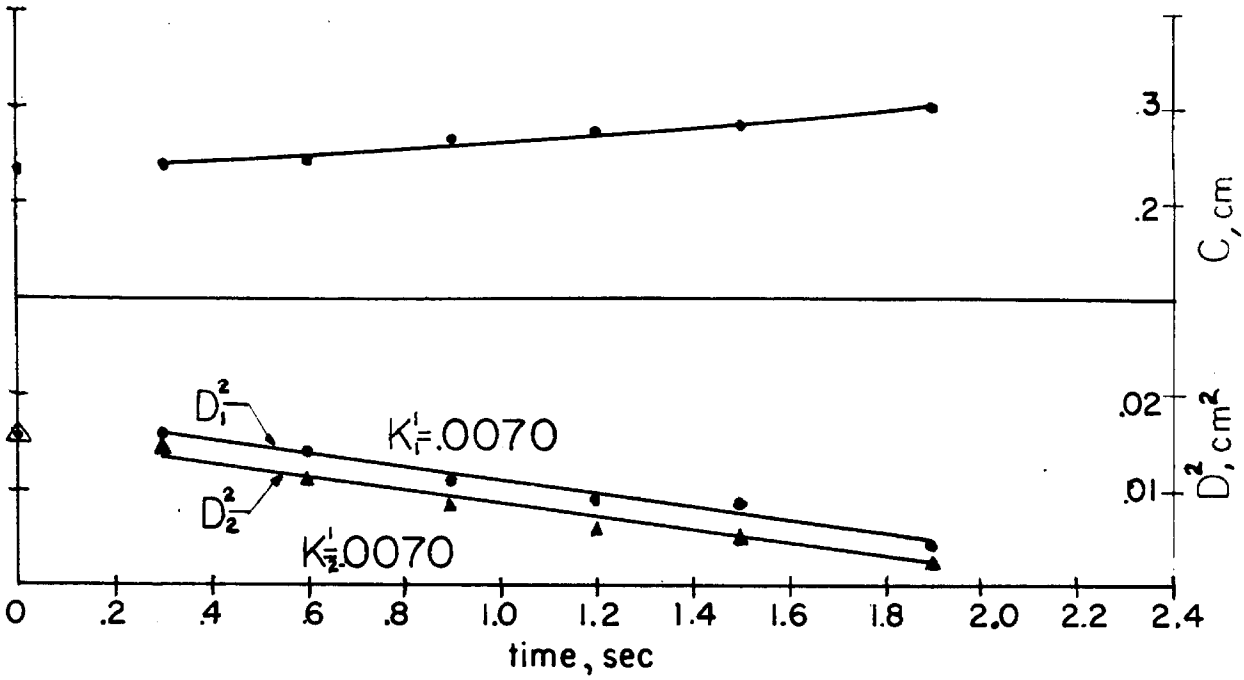

(D_1^o=0.124cm, D_2^o= 0.124cm, C^o= 0.235cm)

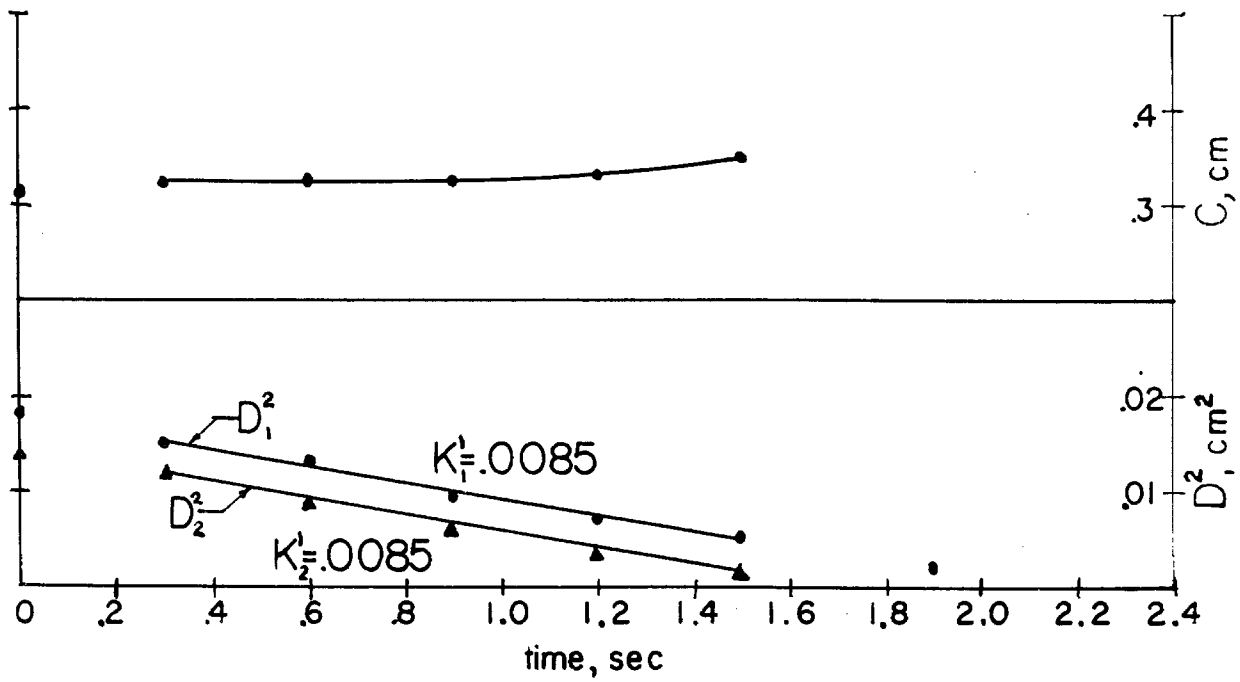

(D_1^o= 0.135cm, D_2^o= 0.117cm, C^o= 0.313cm)

FIGURE 12. PLOTS OF D^2 vs time and C vs time FOR TWO n-HEPTANE DROPLETS BURNING IN STILL AIR FOR VARIOUS C^o

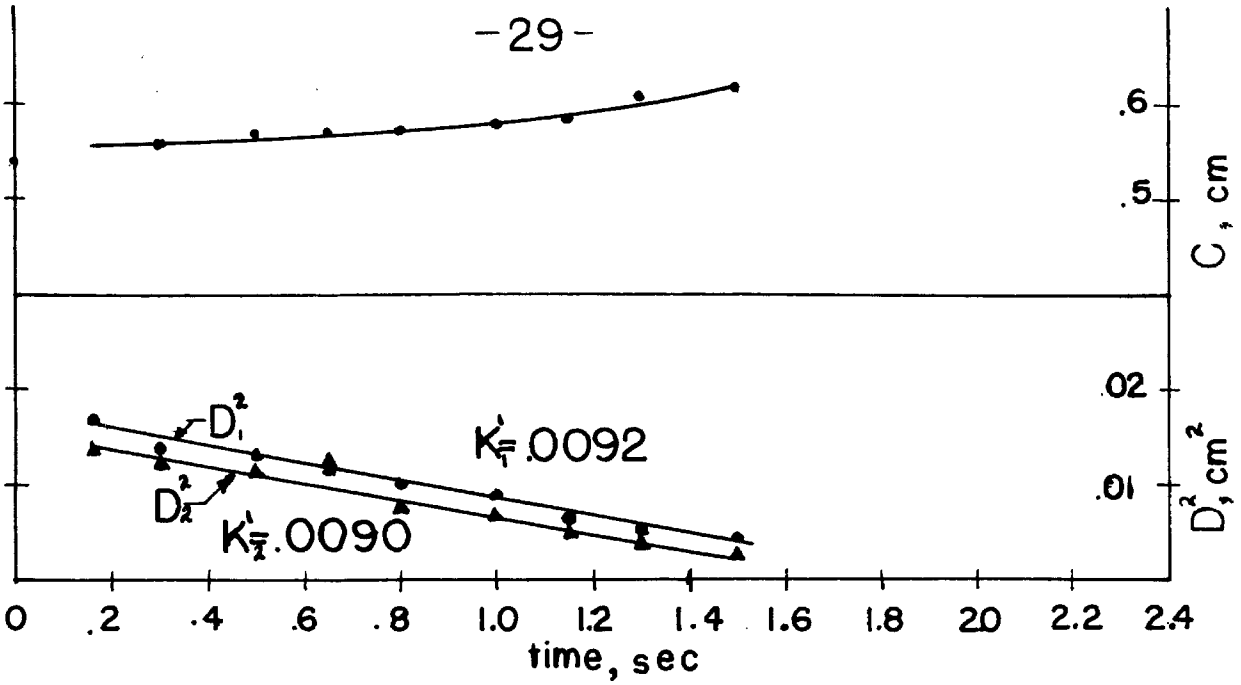

(D_1^o=.133 cm, D_2^o=.122cm, C^o=.540 cm)

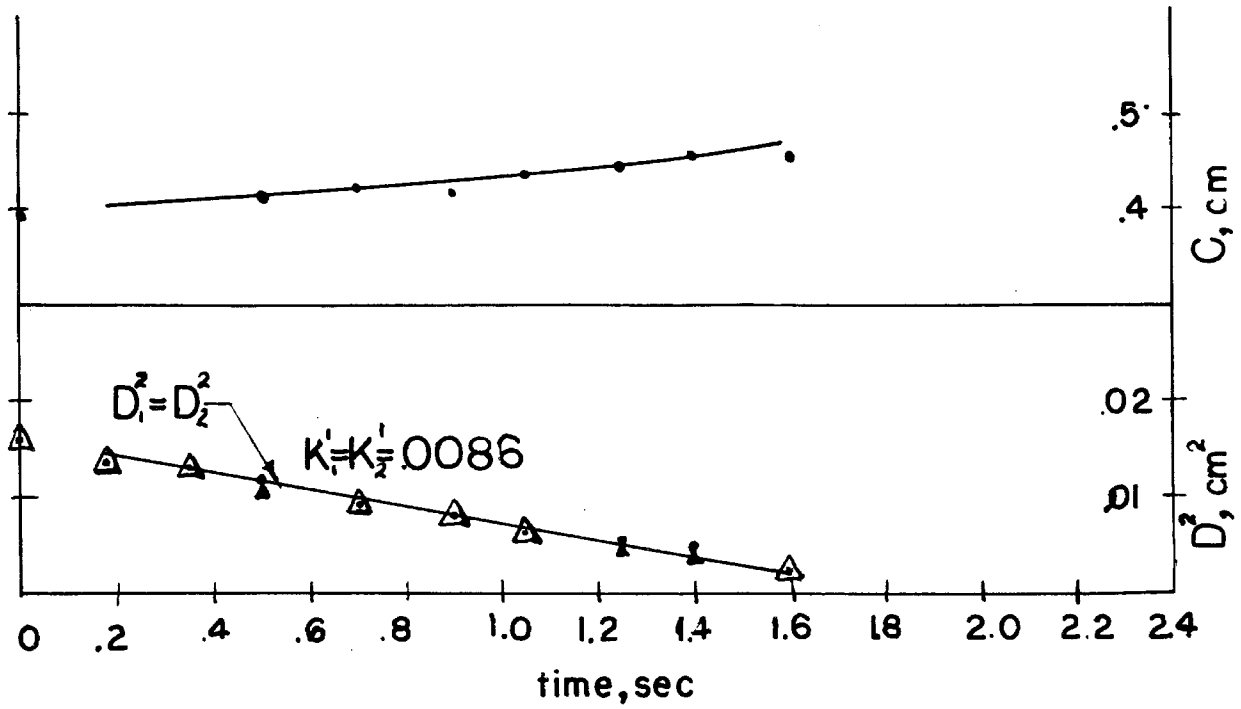

(D_1^o=.126cm, D_2^o=.126cm, C^o=0.40cm)

FIGURE 13. PLOTS OF D^2 vs time and C vs time FOR TWO n-HEPTANE DROPLETS BURNING IN STILL AIR FOR VARIOUS C^o

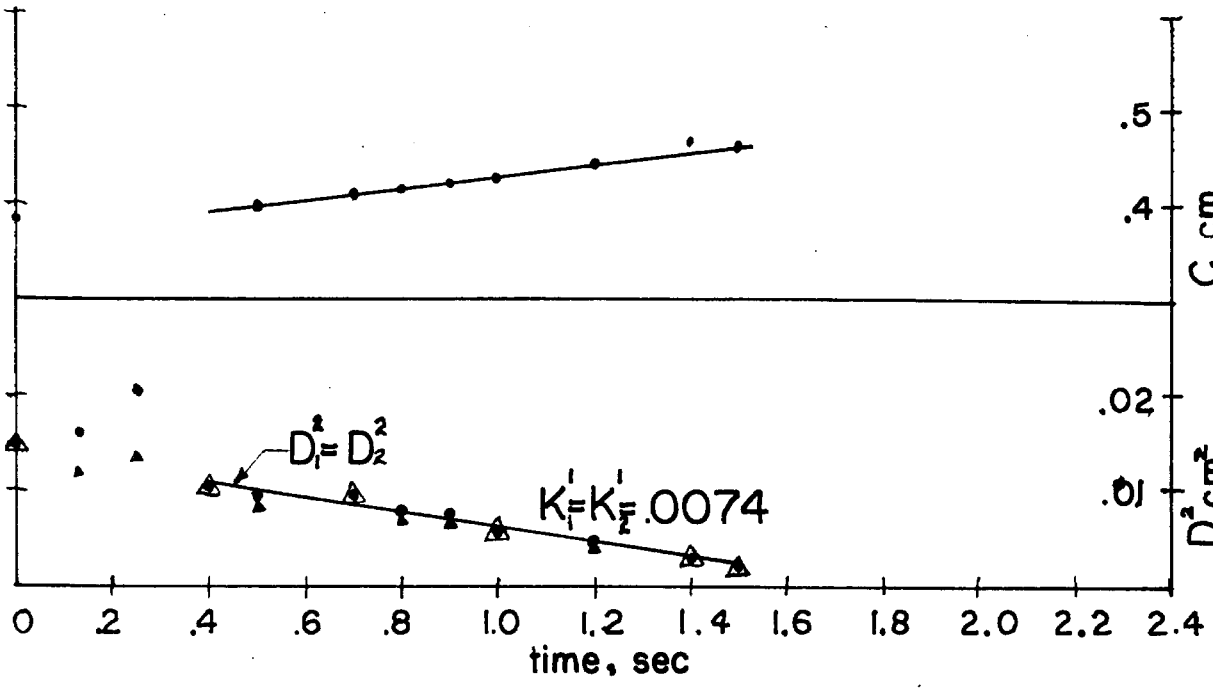

$(D_1^o = 0.121\,cm,\ D_2^o = 0.118\,cm,\ C^o = 0.384\,cm)$

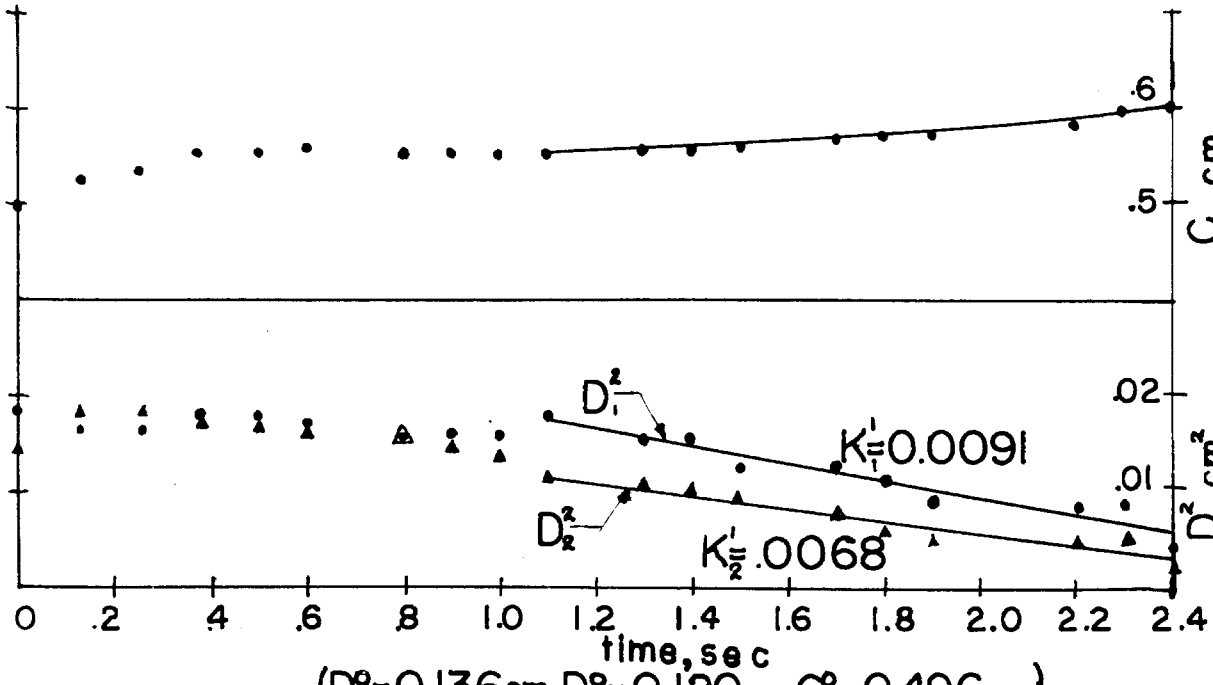

$(D_1^o = 0.136\,cm, D_2^o = 0.120\,cm, C^o = 0.496\,cm)$

FIGURE 14. PLOTS OF D^2 vs time and C vs time FOR TWO n-HEPTANE DROPLETS BURNING IN STILL AIR FOR VARIOUS C^o

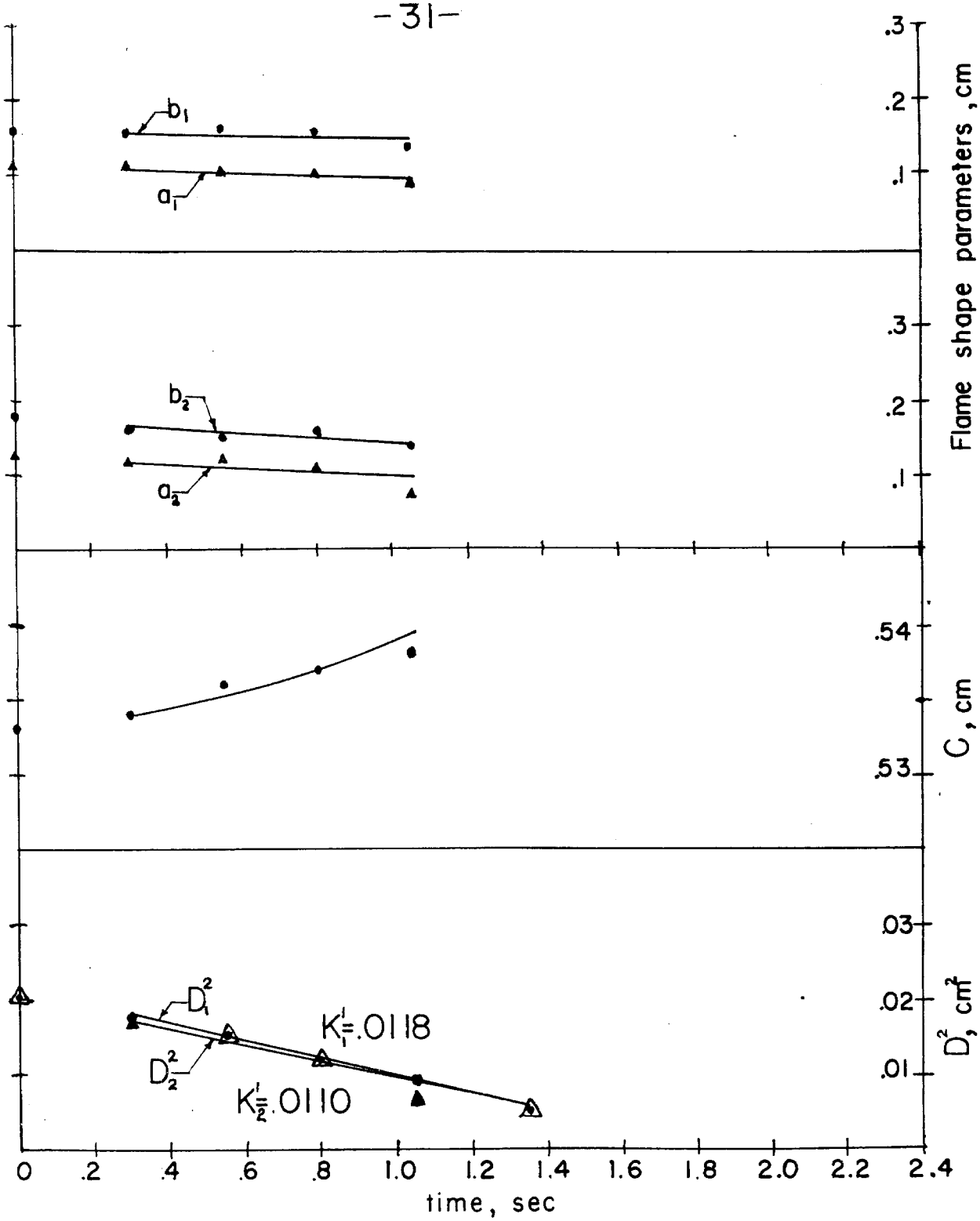

FIGURE 15. EXPERIMENTAL RESULTS FOR TWO n-HEPTANE DROPLETS BURNING IN STILL AIR (D_1°=0.143 cm, D_2°=0.142cm, C°=0.533 cm)

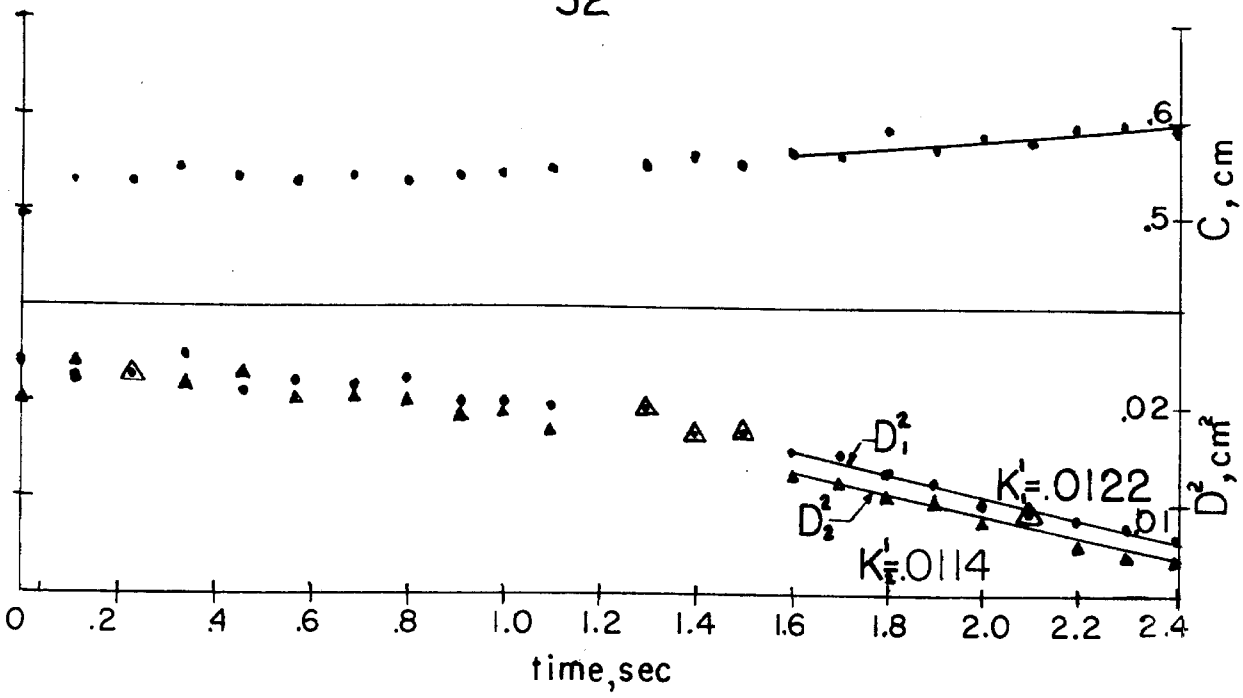

(D_1^o=0.155cm, D_2^o=0.142cm, C^o=0.496cm)

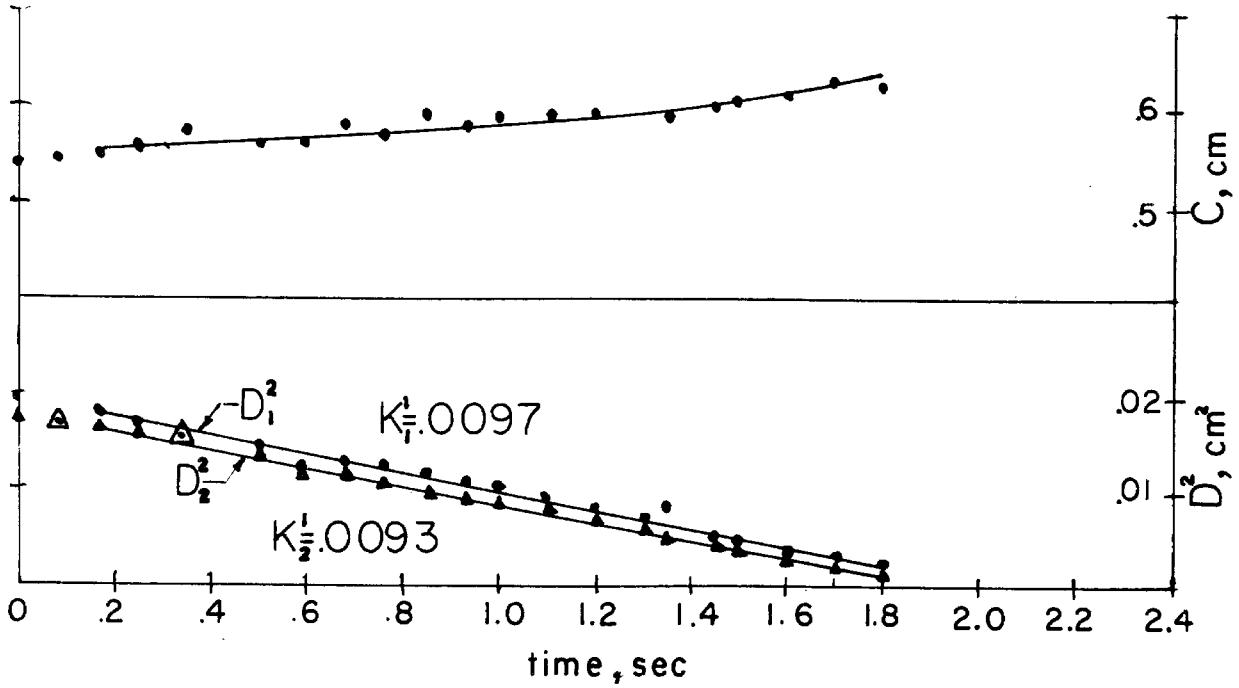

(D_1^o=0.141cm, D_2^o=0.135cm, C^o=0.538cm)

FIGURE 16. PLOTS OF D^2 vs time and C vs time FOR TWO n-HEPTANE DROPLETS BURNING IN STILL AIR FOR VARIOUS C^o

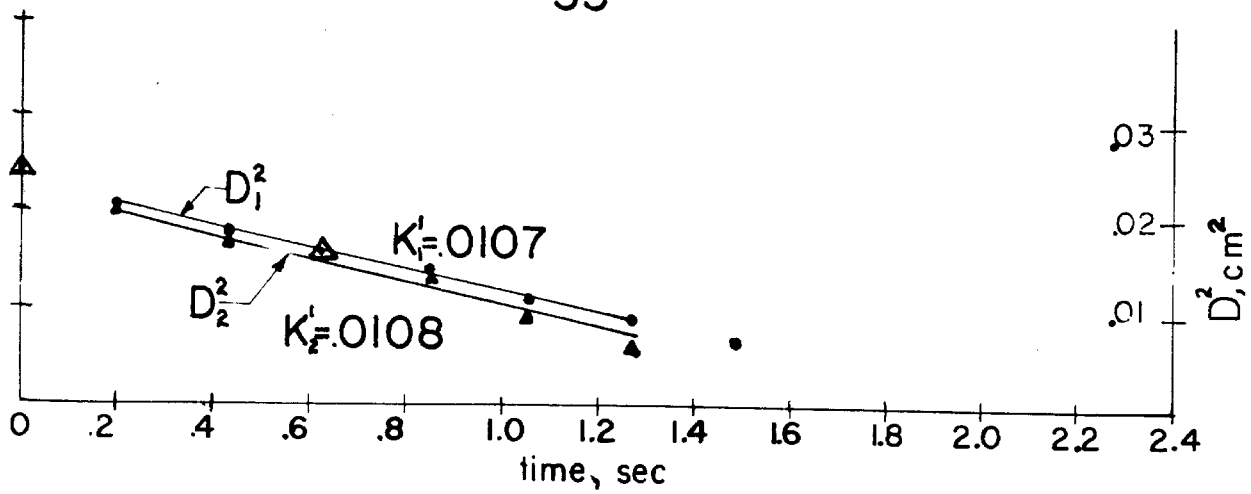

(D_1^o=0.156cm, D_2^o=0.156cm, C^o=1.10cm)

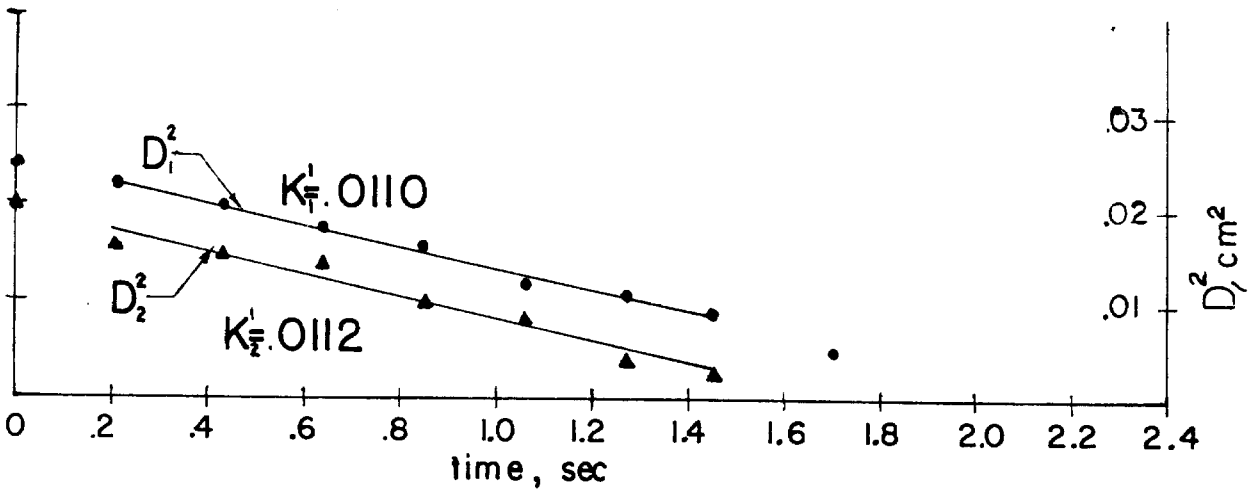

(D_1^o=0.156cm, D_2^o=0.141cm, C^o=0.883cm)

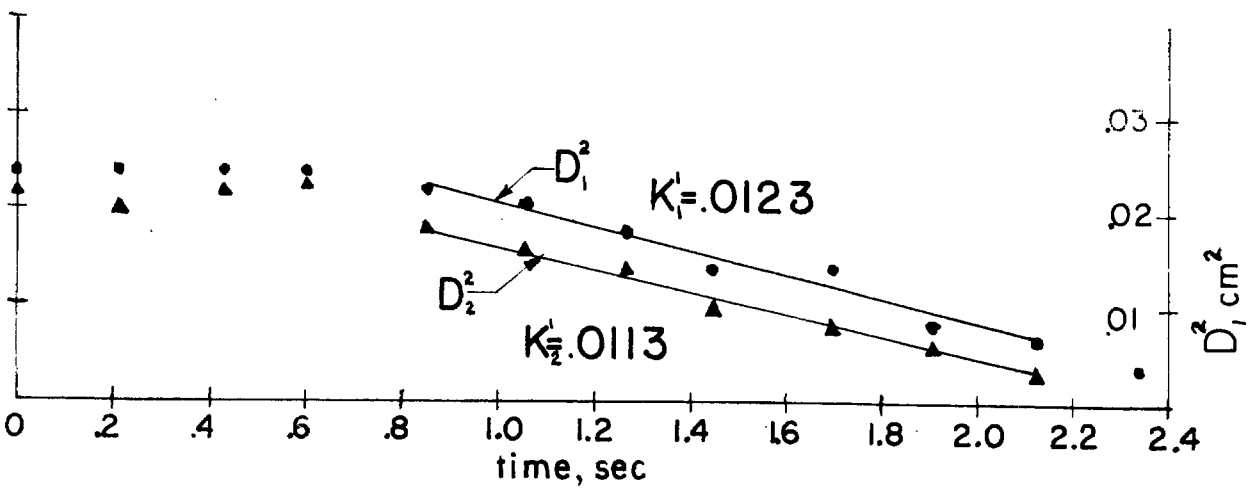

(D_1^o=0.156cm, D_2^o=0.147cm, C^o=0.813cm)

FIGURE 17. PLOTS OF D^2 vs time FOR TWO n-HEPTANE DROPLETS BURNING IN STILL AIR FOR VARIOUS C^o

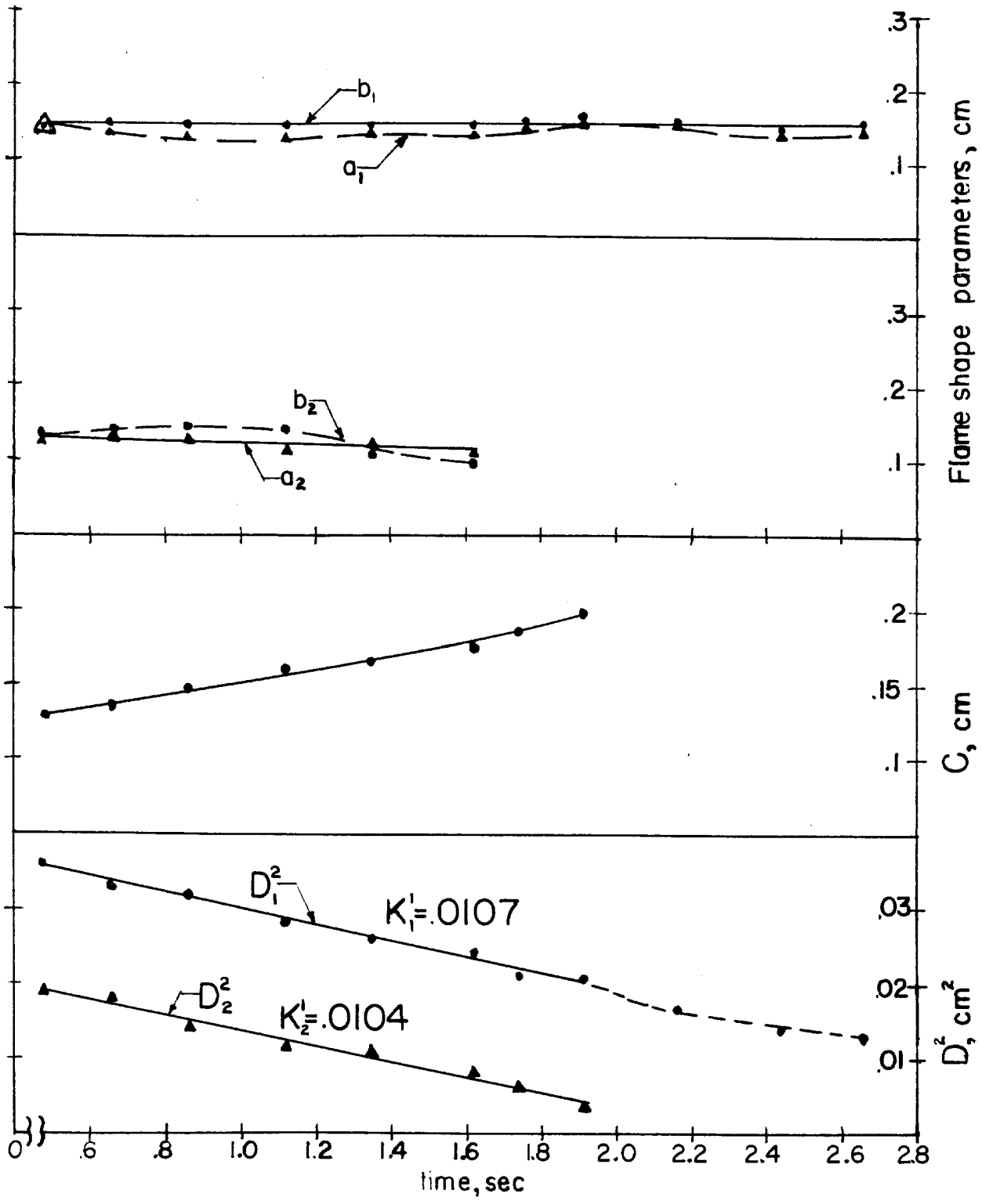

FIGURE 18. EXPERIMENTAL RESULTS FOR TWO n-HEPTANE DROPLETS BURNING IN STILL AIR (D_1^o=0.208 cm, D_2^o=0.155cm, C^o=0.126cm)

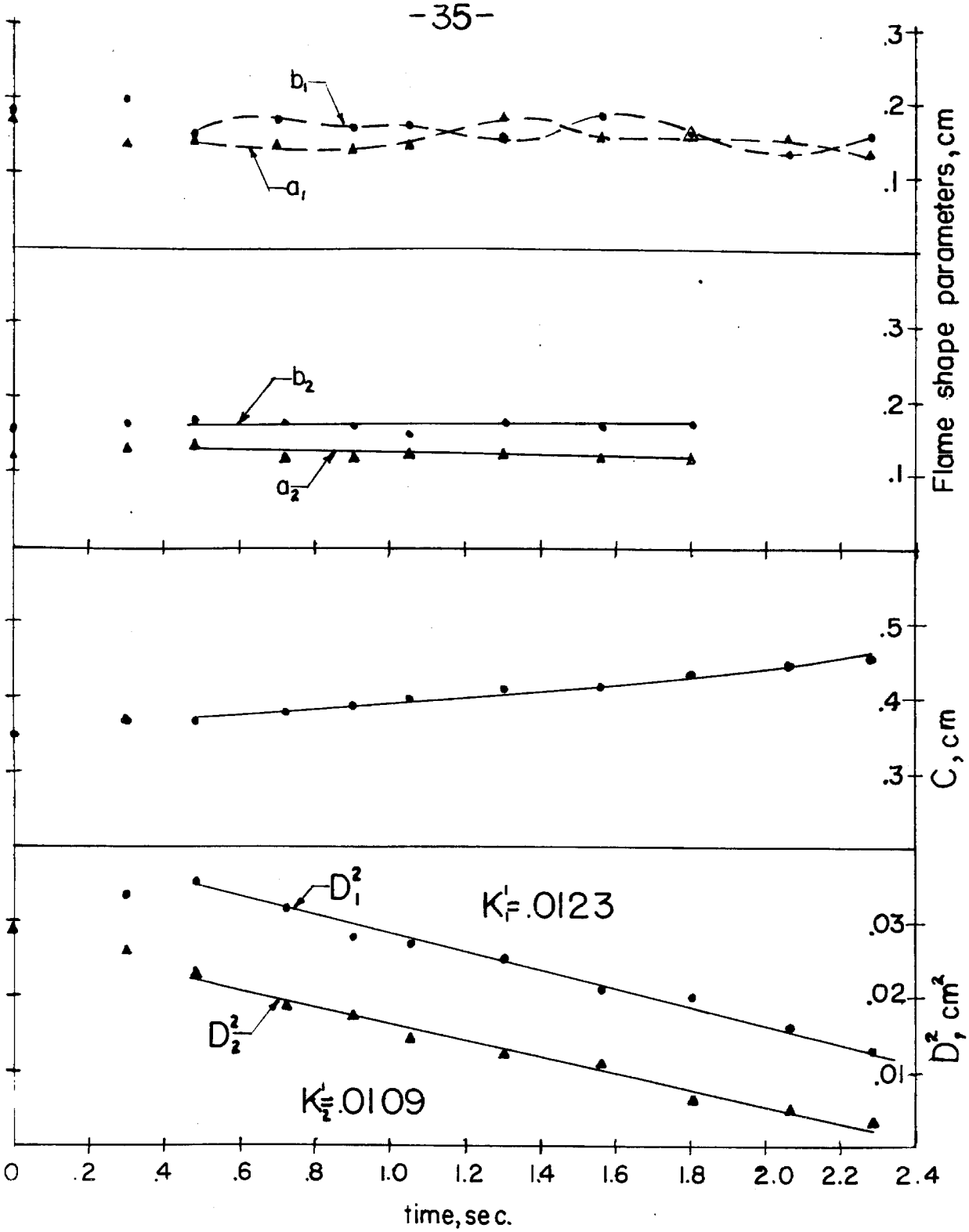

FIGURE 19. EXPERIMENTAL RESULTS FOR TWO n-HEPTANE DROPLETS BURNING IN STILL AIR (D_1^o=0.209 cm, D_2^o=0.170cm, C^o=0.352cm)

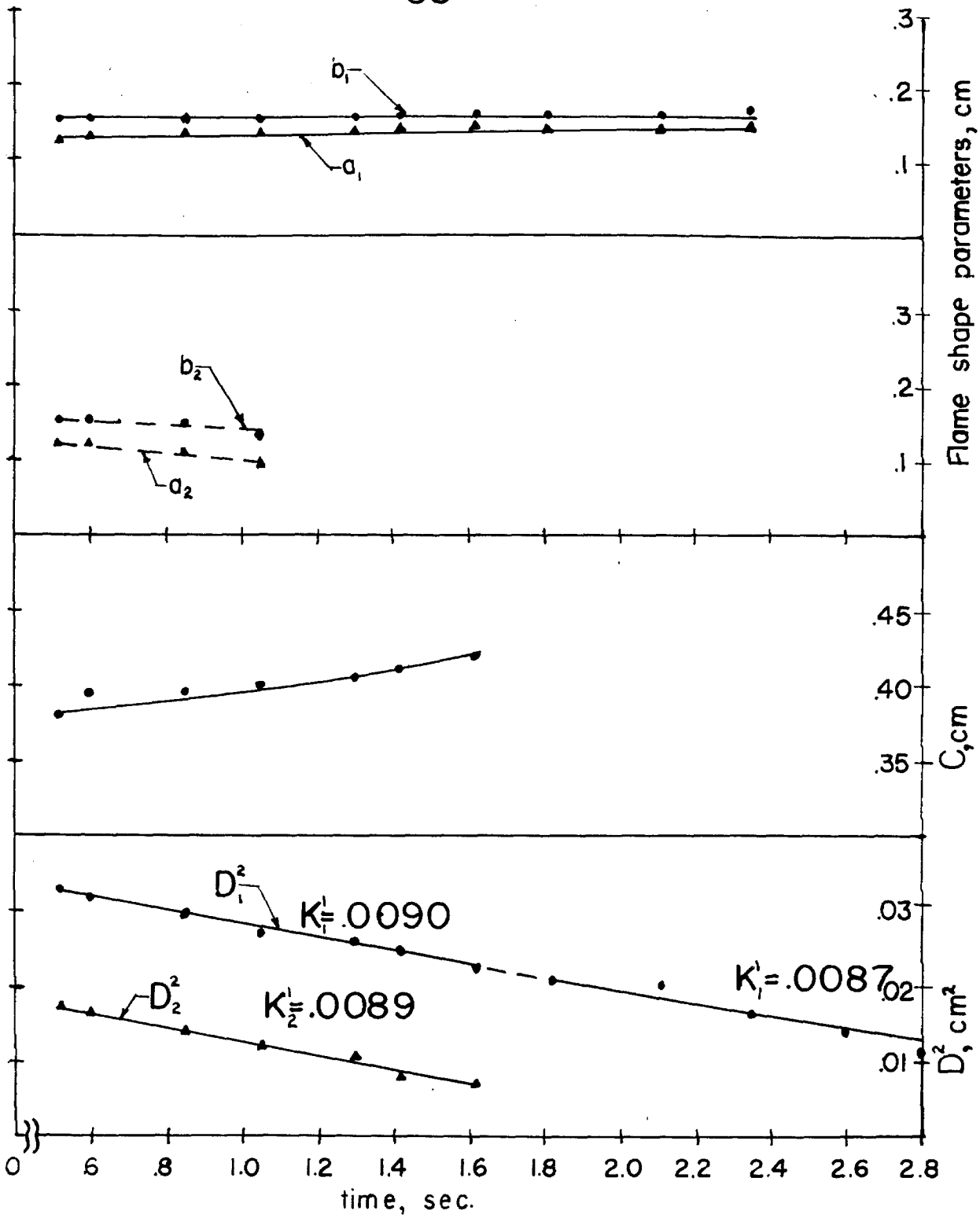

FIGURE 20. EXPERIMENTAL RESULTS FOR TWO n-HEPTANE DROPLETS BURNING IN STILL AIR (D_1^o= 0.198 cm, D_2^o=0.140cm, C^o=0.375cm)

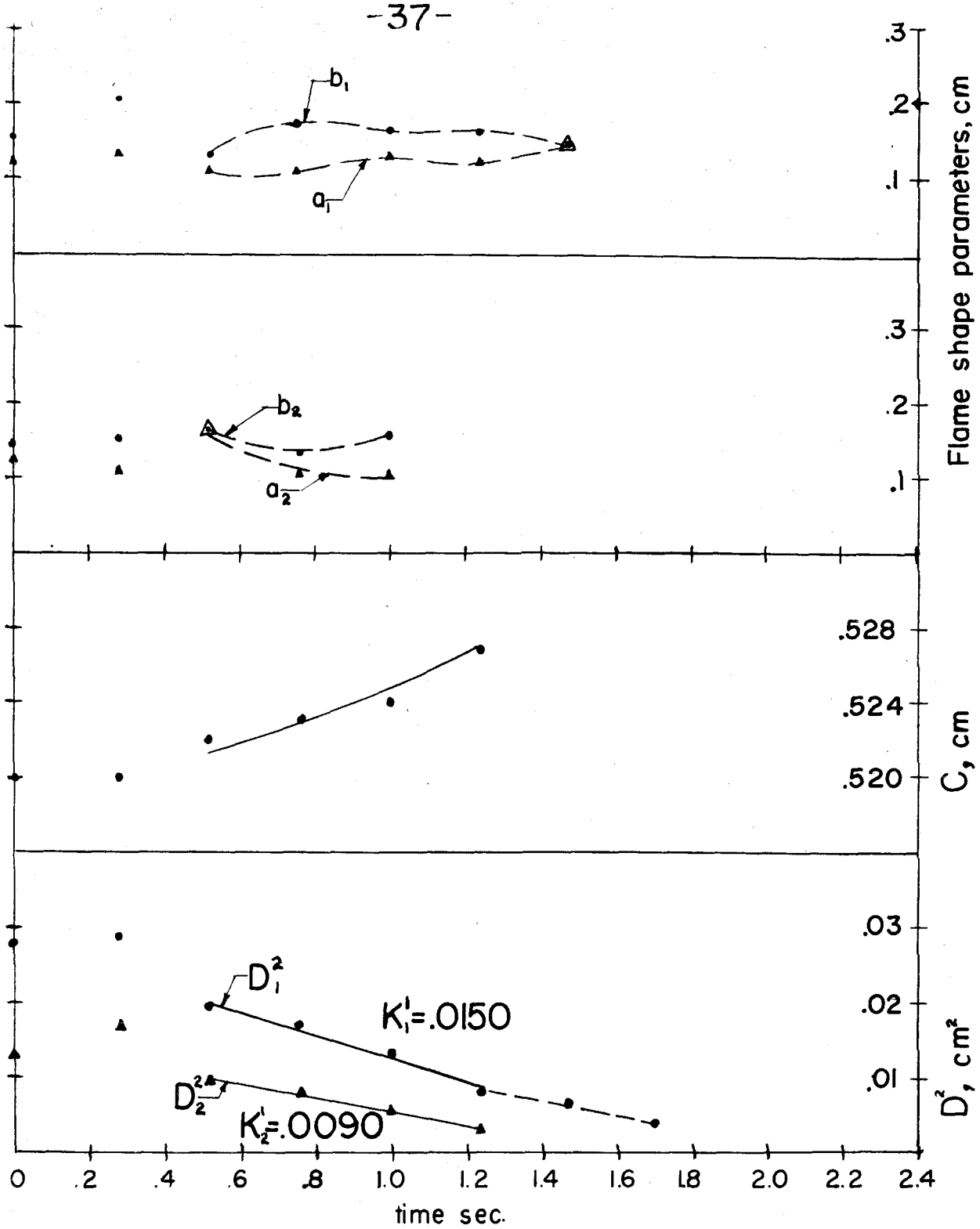

FIGURE 21. EXPERMENTAL RESULTS FOR TWO n-HEPTANE DROPLETS BURNING IN STILL AIR (D_1^o= 0.167 cm, D_2^o= 0.115 cm, C^o = 0.520 cm)

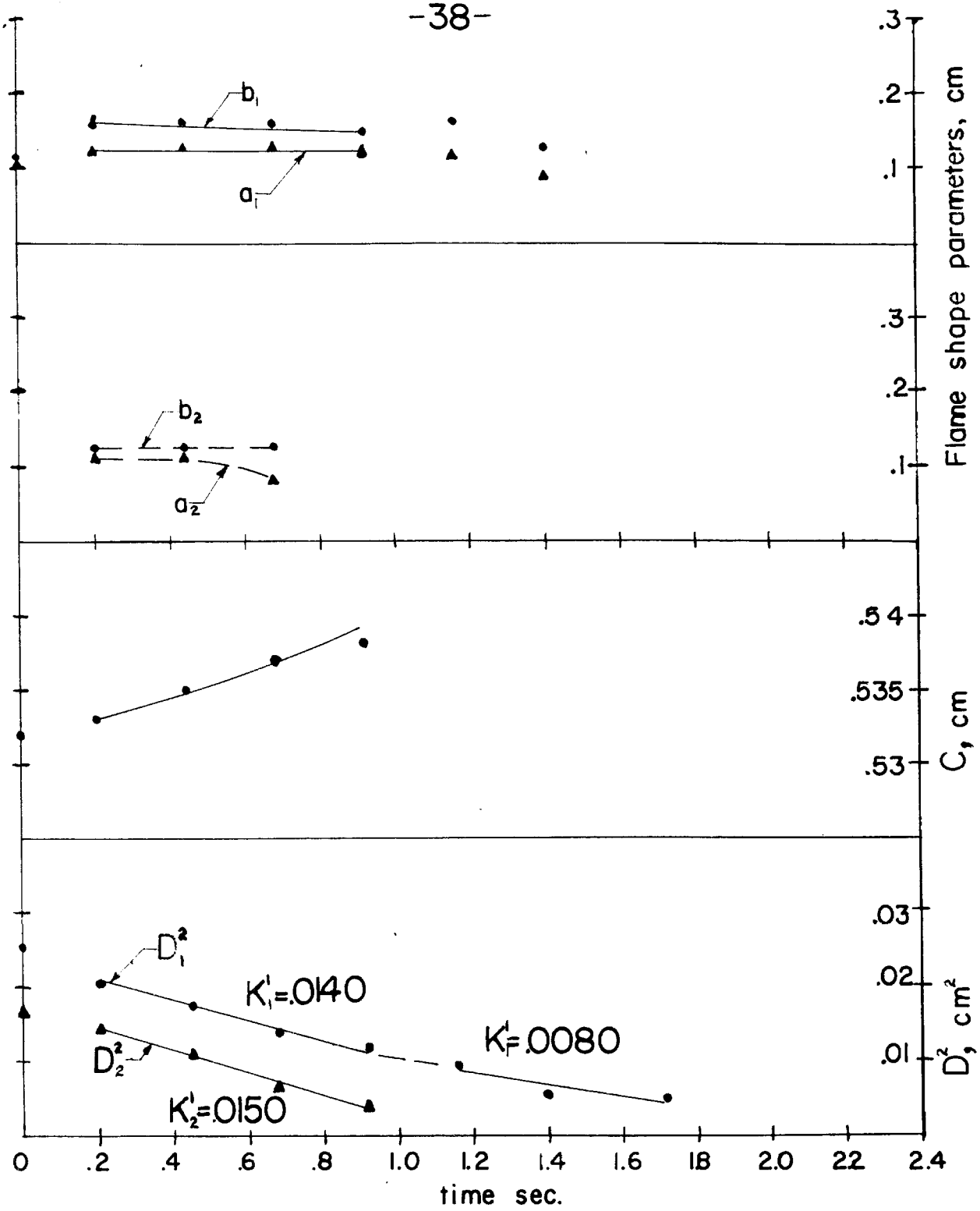

FIGURE 22. EXPERIMENTAL RESULTS FOR TWO n-HEPTANE DROPLETS BURNING IN STILL AIR (D_1^o=0.160 cm, D_2^o=0.131 cm, C^o=0.532 cm)

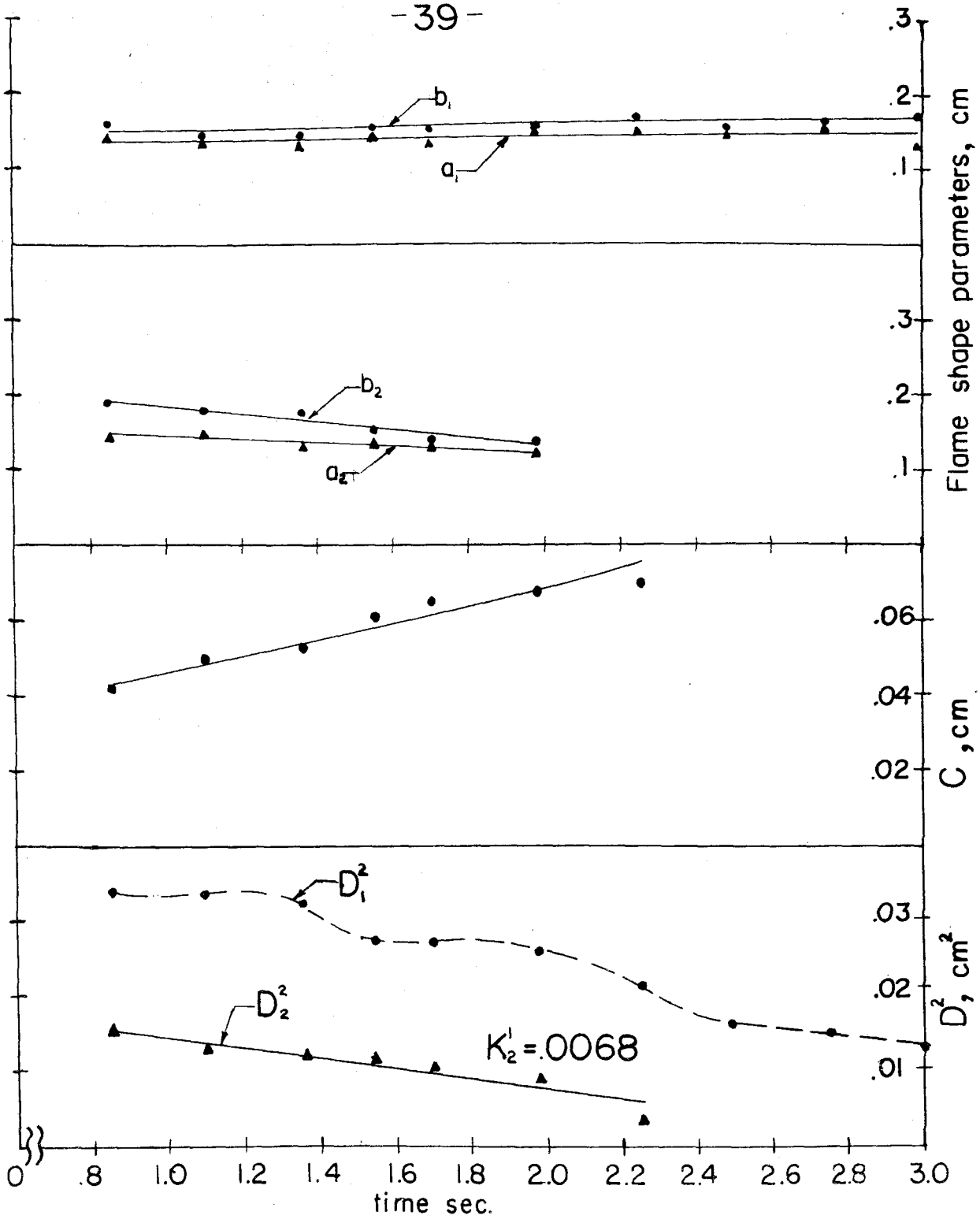

FIGURE 23. EXPERIMENTAL RESULTS FOR TWO *n*-HEPTANE DROPLETS BURNING IN STILL AIR (D_1^o=0.192 cm, D_2^o=0.148 cm, C^o=0.026 cm)

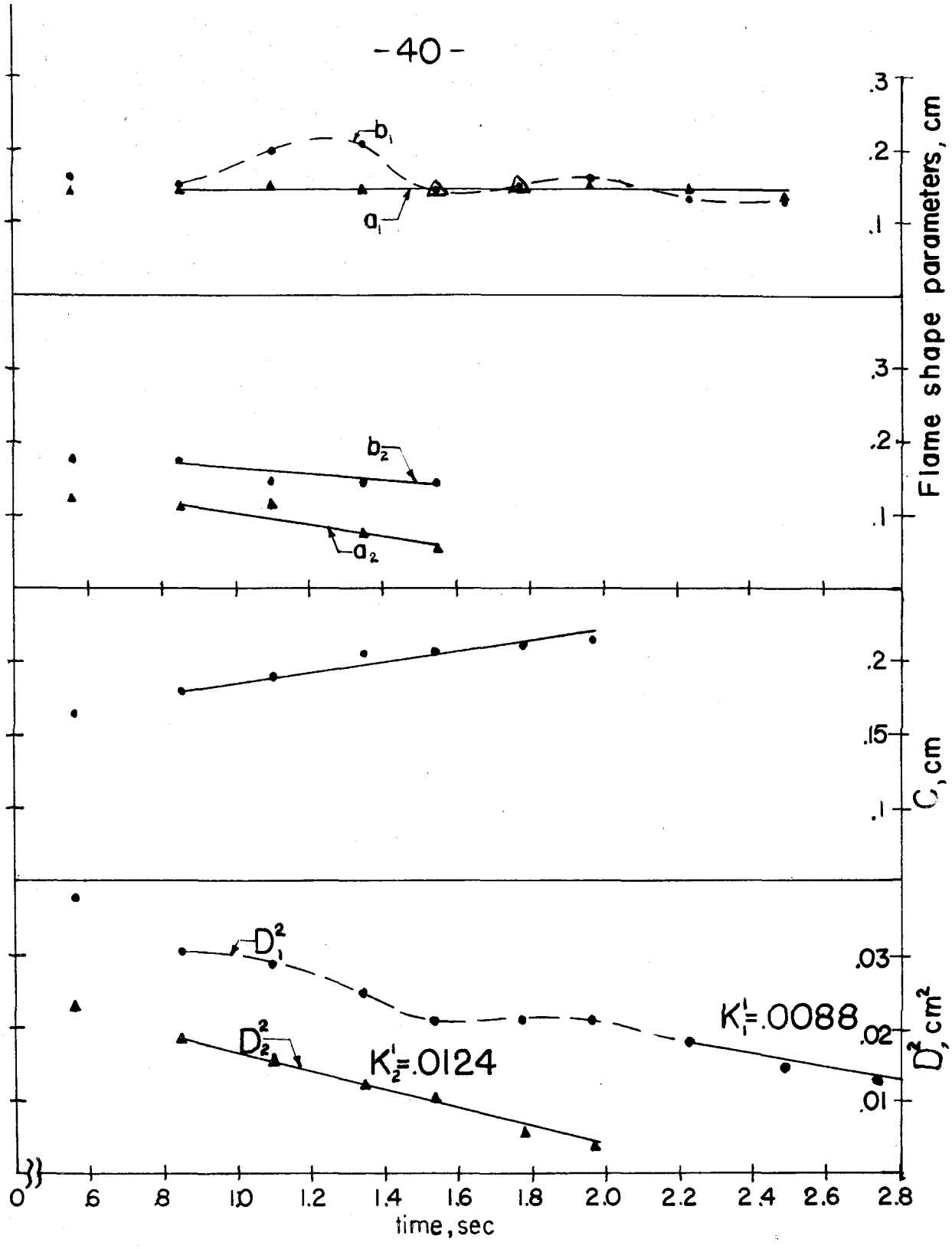

FIGURE 24. EXPERIMENTAL RESULTS FOR TWO n-HEPTANE DROPLETS BURNING IN STILL AIR (D_1^o=0.208 cm, D_2^o=0.164cm, C^o=0.150cm)

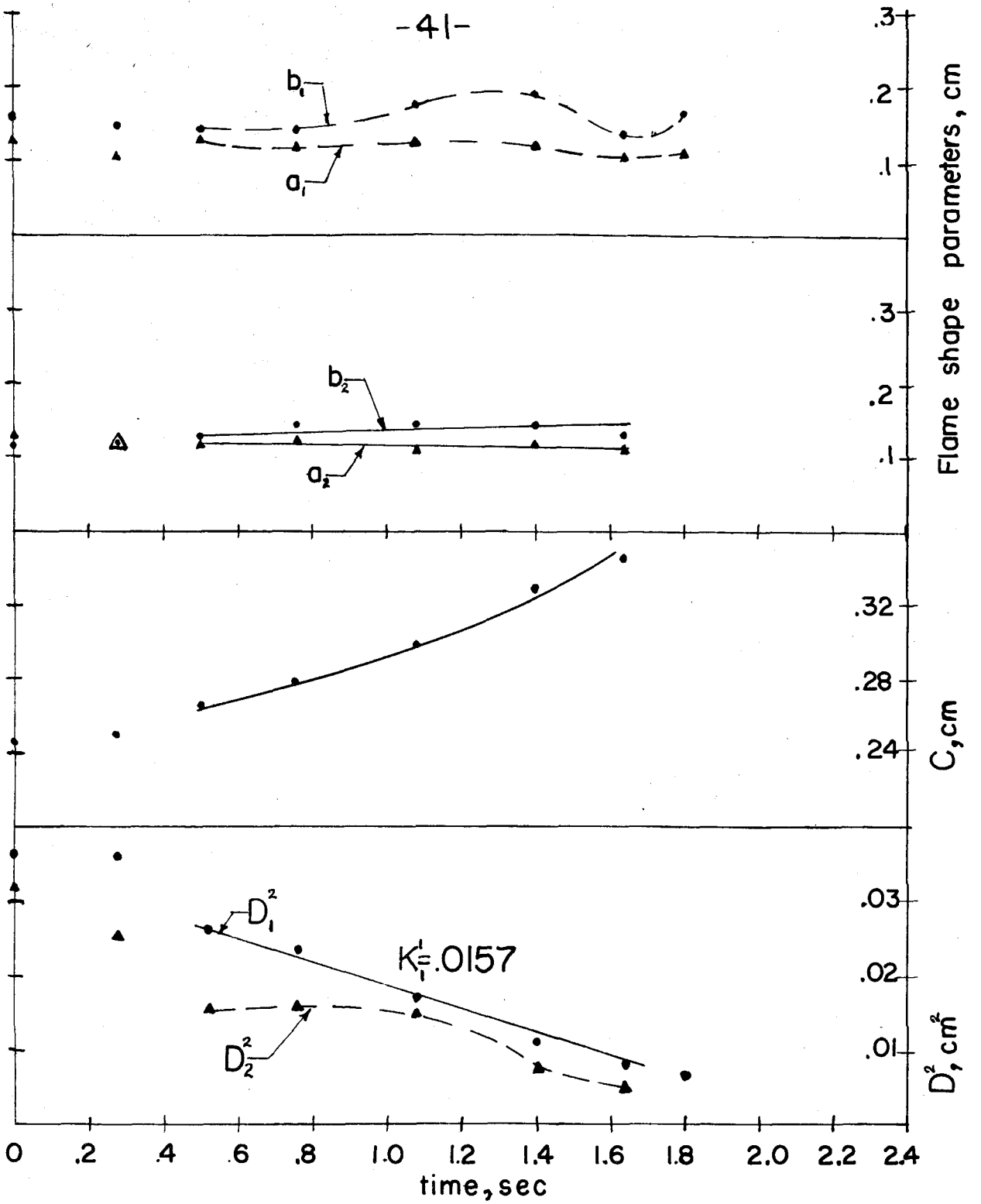

FIGURE 25. EXPERIMENTAL RESULTS FOR TWO n-HEPTANE DROPLETS BURNING IN STILL AIR (D_1^o = 0.191cm, D_2^o=0.178cm, C^o=0246cm)

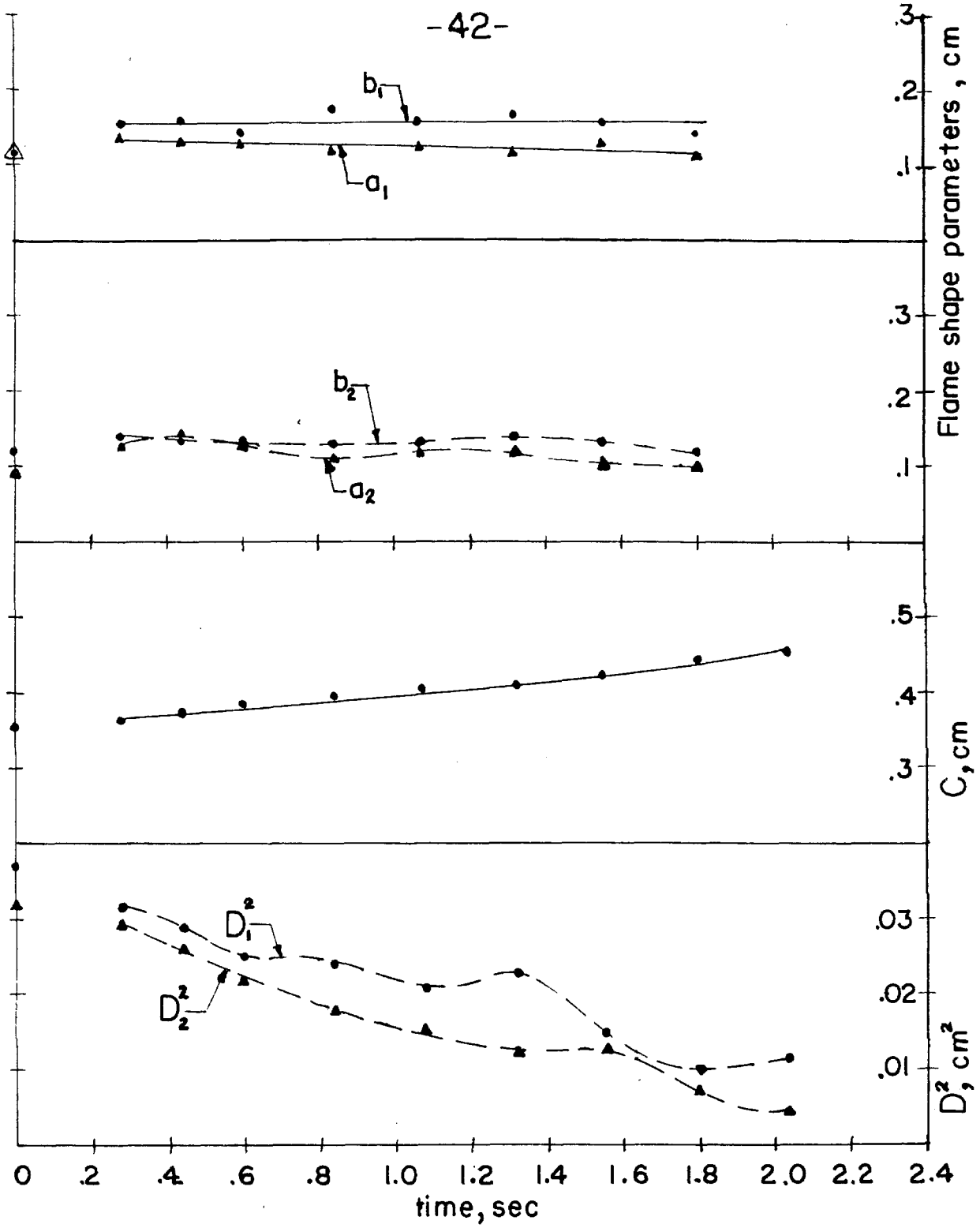

FIGURE 26. EXPERIMENTAL RESULTS FOR TWO n-HEPTANE DROPLETS BURNING IN STILL AIR (D_1^o= 0.192cm, D_2^o=0.180cm, C^o=0.355cm)

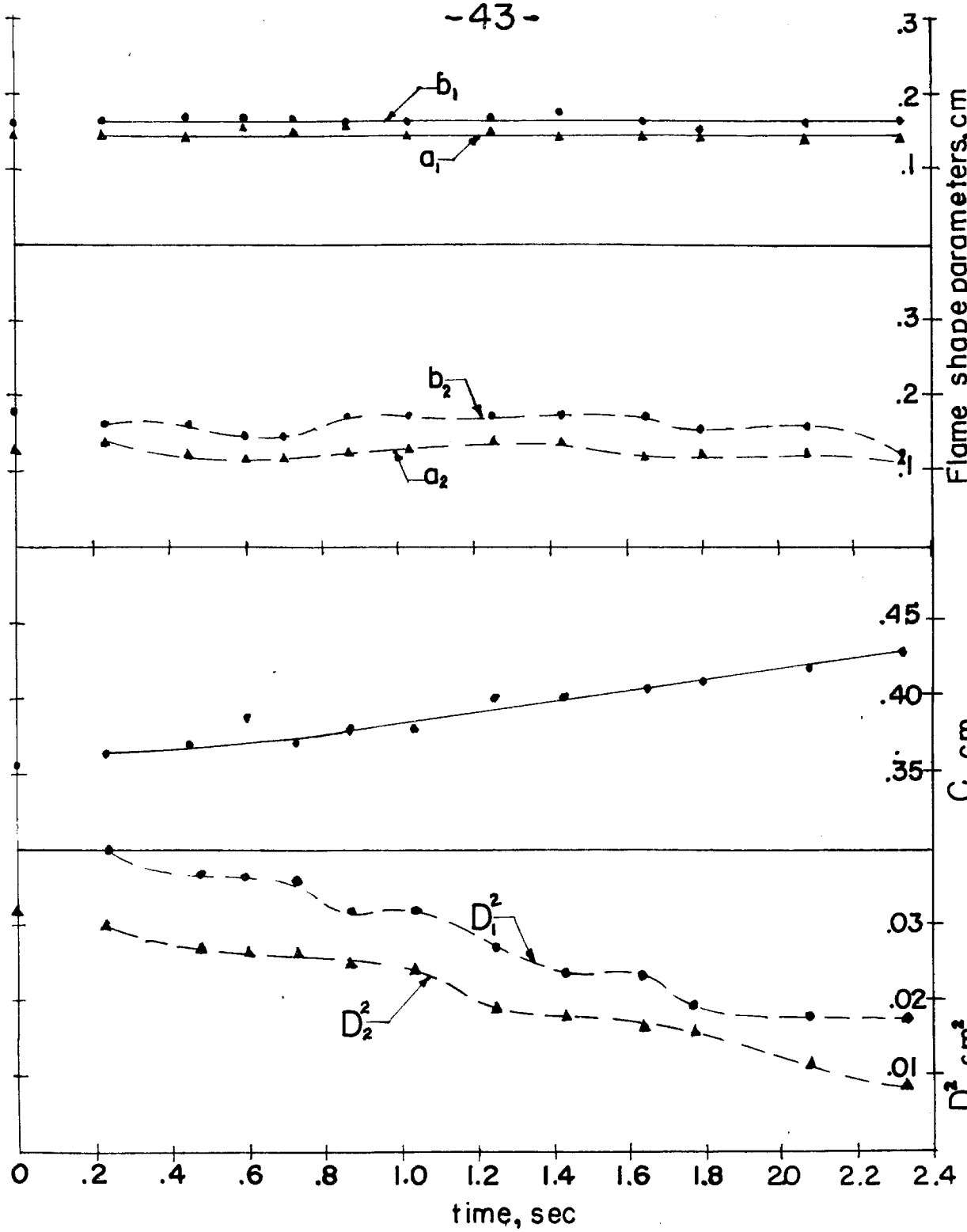

FIGURE 27. EXPERIMENTAL RESULTS FOR TWO n-HEPTANE DROPLETS BURNING IN STILL AIR (D_1^o=0.202 cm, D_2^o=0.179 cm, C^o=0.362 cm)

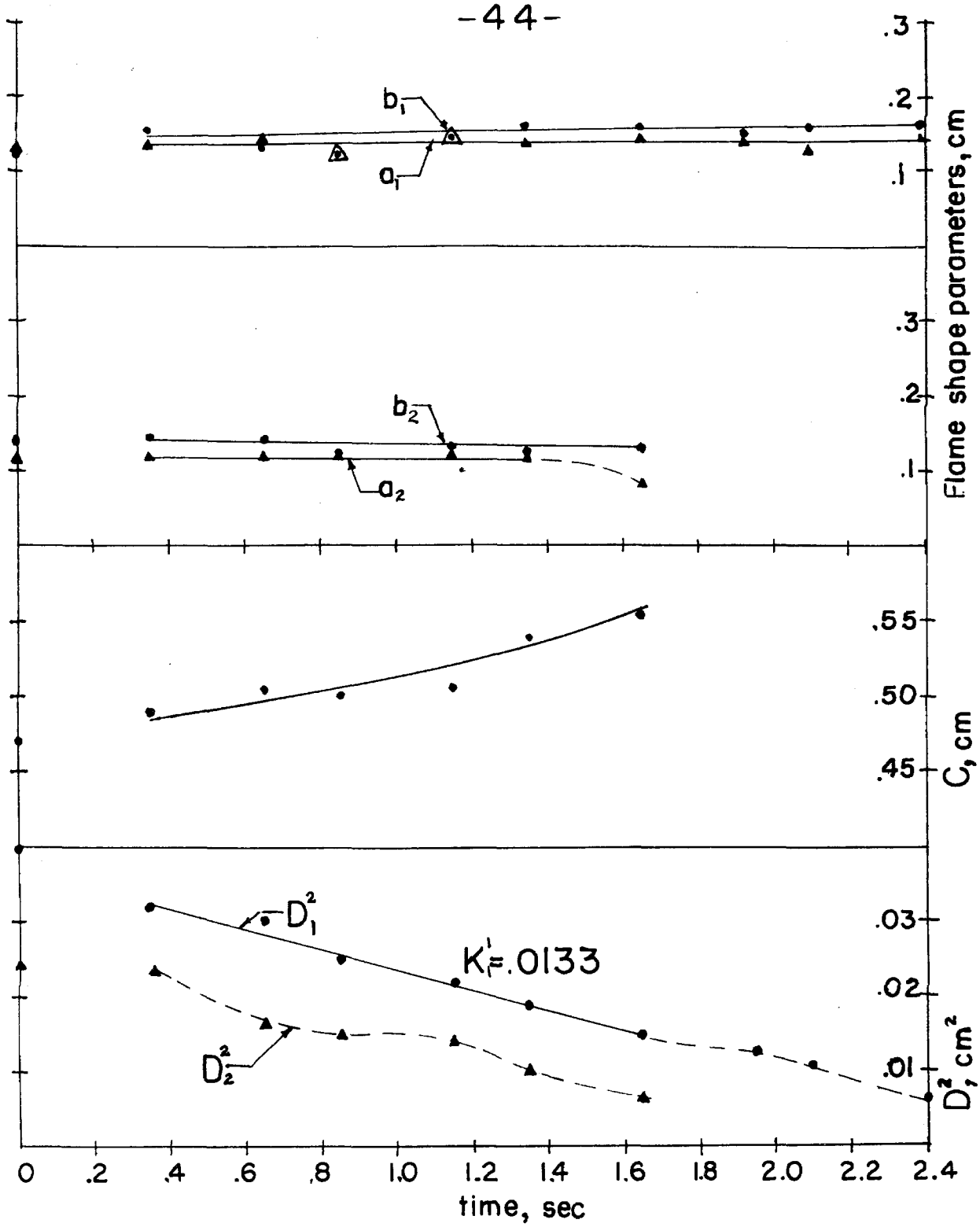

FIGURE 28. EXPERIMENTAL RESULTS FOR TWO n-HEPTANE DROPLETS BURNING IN STILL AIR (D_1^o= 0.200 cm, D_2^o=0.156 cm, C^o= 0.466cm)

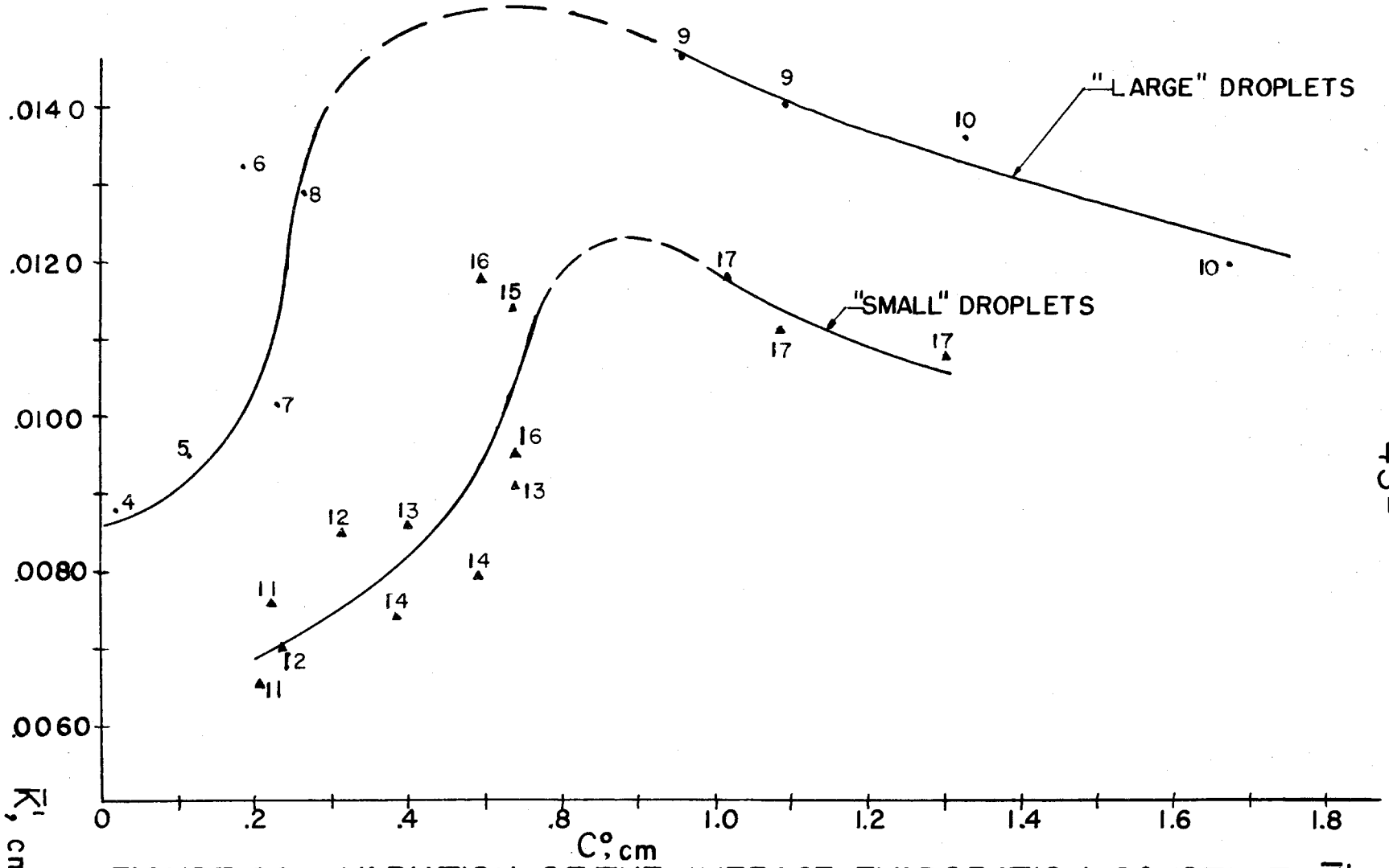

FIGURE 29. VARIATION OF THE AVERAGE EVAPORATION CONSTANT $\bar{K}'$ WITH C° FOR DROPLET PAIRS WITH DIFFERENT INITIAL AVERAGE DIAMETERS $\bar{D}°$

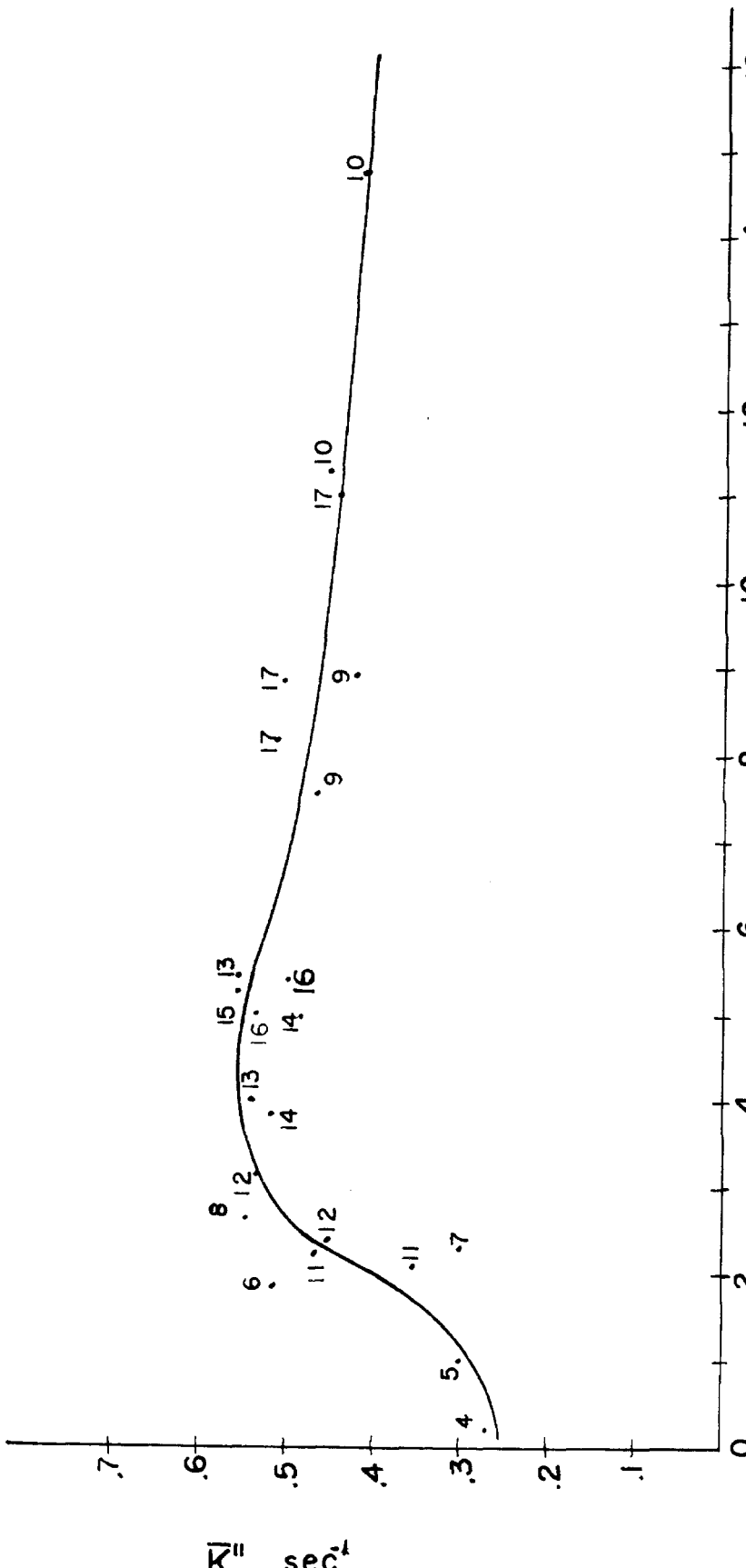

FIGURE 30. DEPENDENCE OF THE EVAPORATION FREQUENCY $\bar{K}''$ ON C°

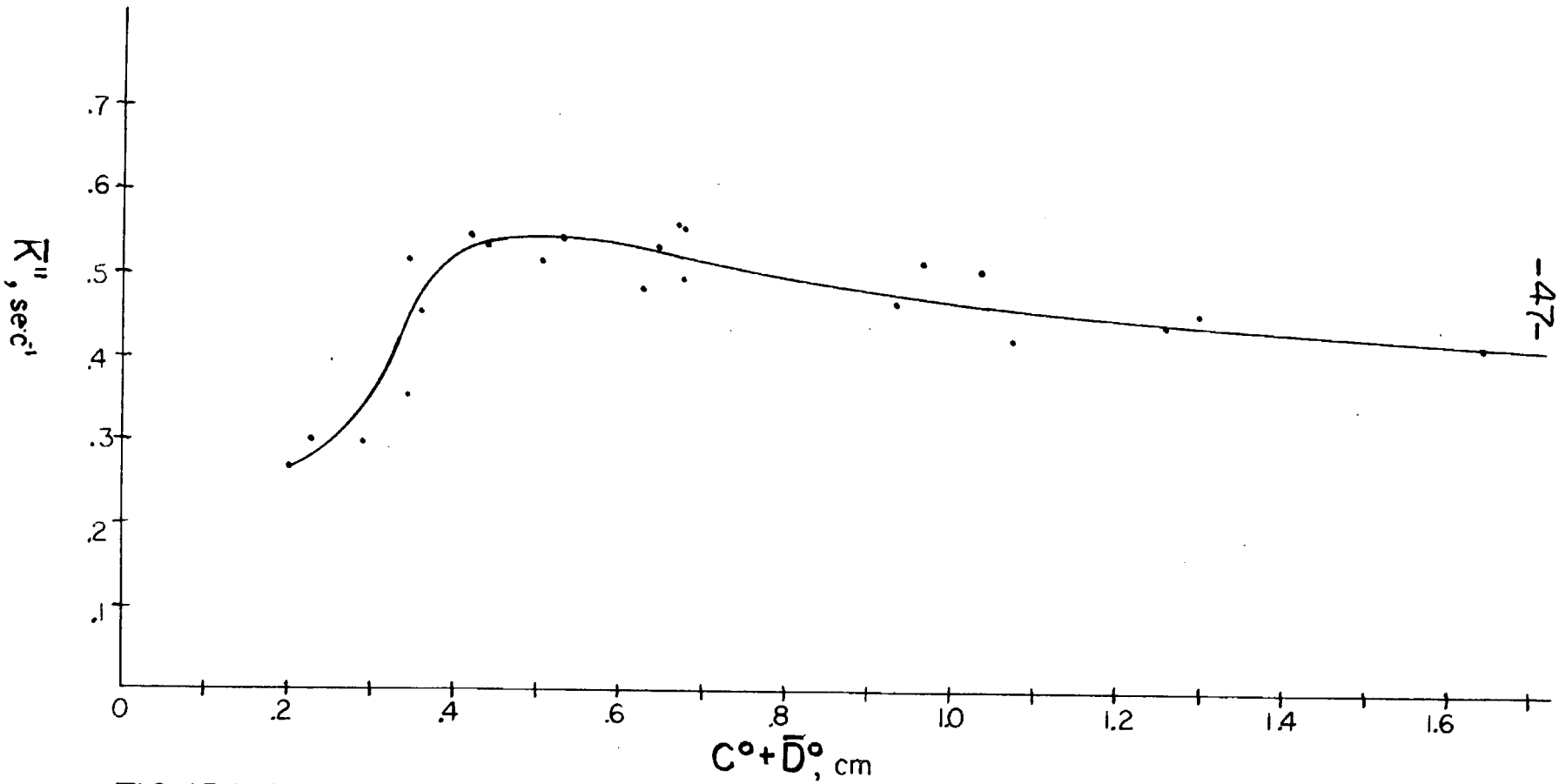

FIGURE 31. DEPENDENCE OF THE EVAPORATION FREQUENCY $\bar{K}''$ ON $C^\circ + \bar{D}^\circ$

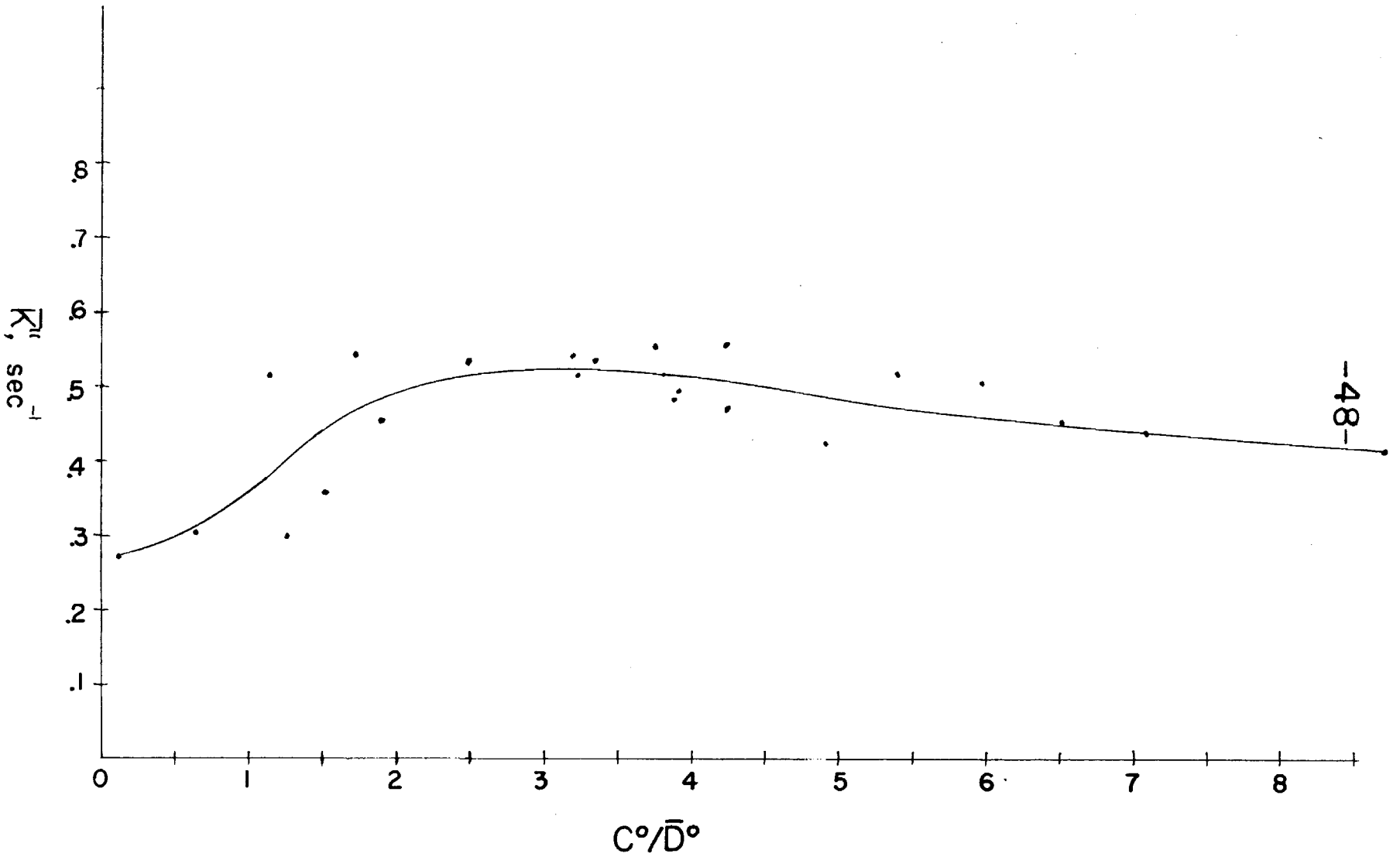

FIGURE 32. DEPENDENCE OF THE EVAPORATION FREQUENCY $\bar{K}''$ ON $C°/\bar{D}°$

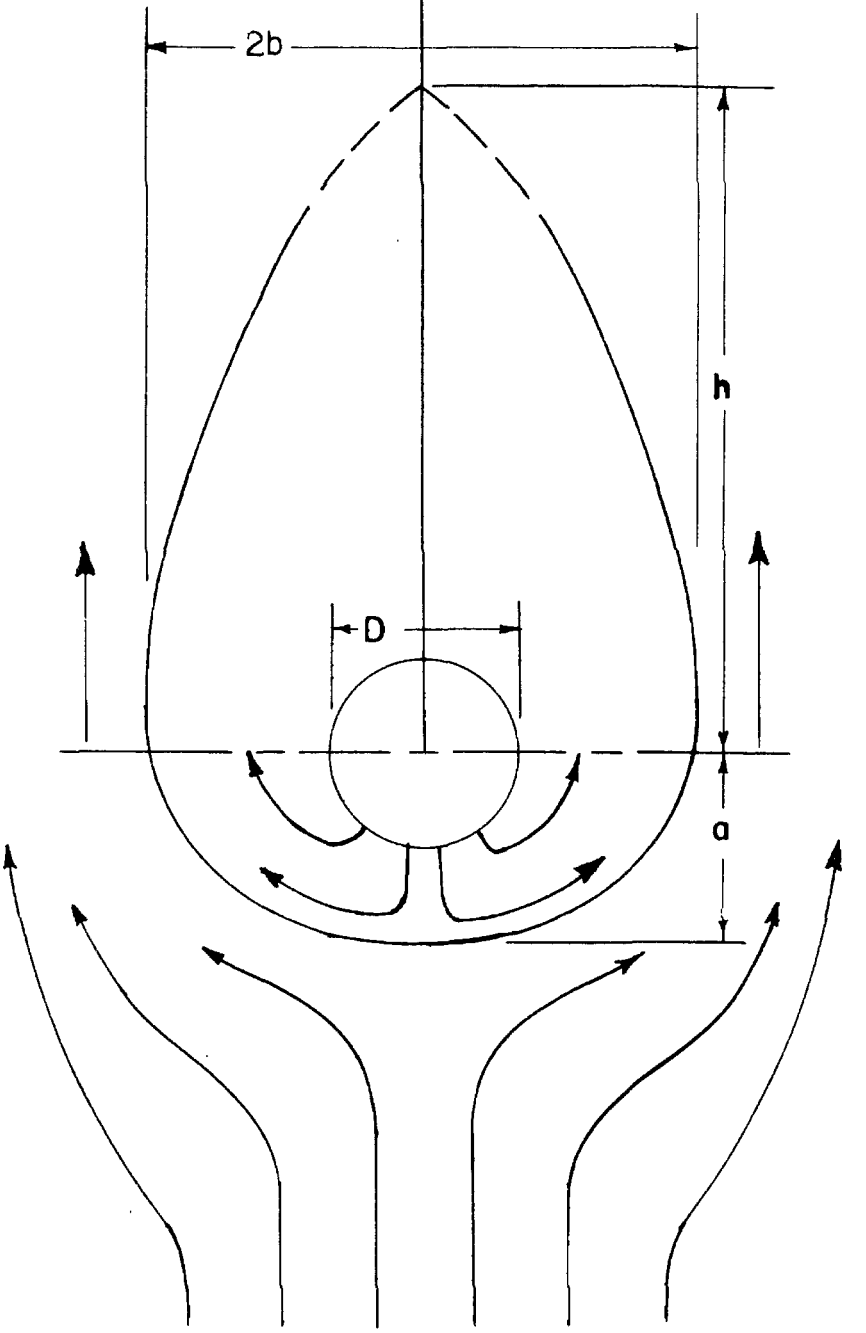

FIGURE 33. SCHEMATIC DIAGRAM OF BURNING FUEL DROPLET. STREAMLINES IDENTIFIED BY ARROWS.

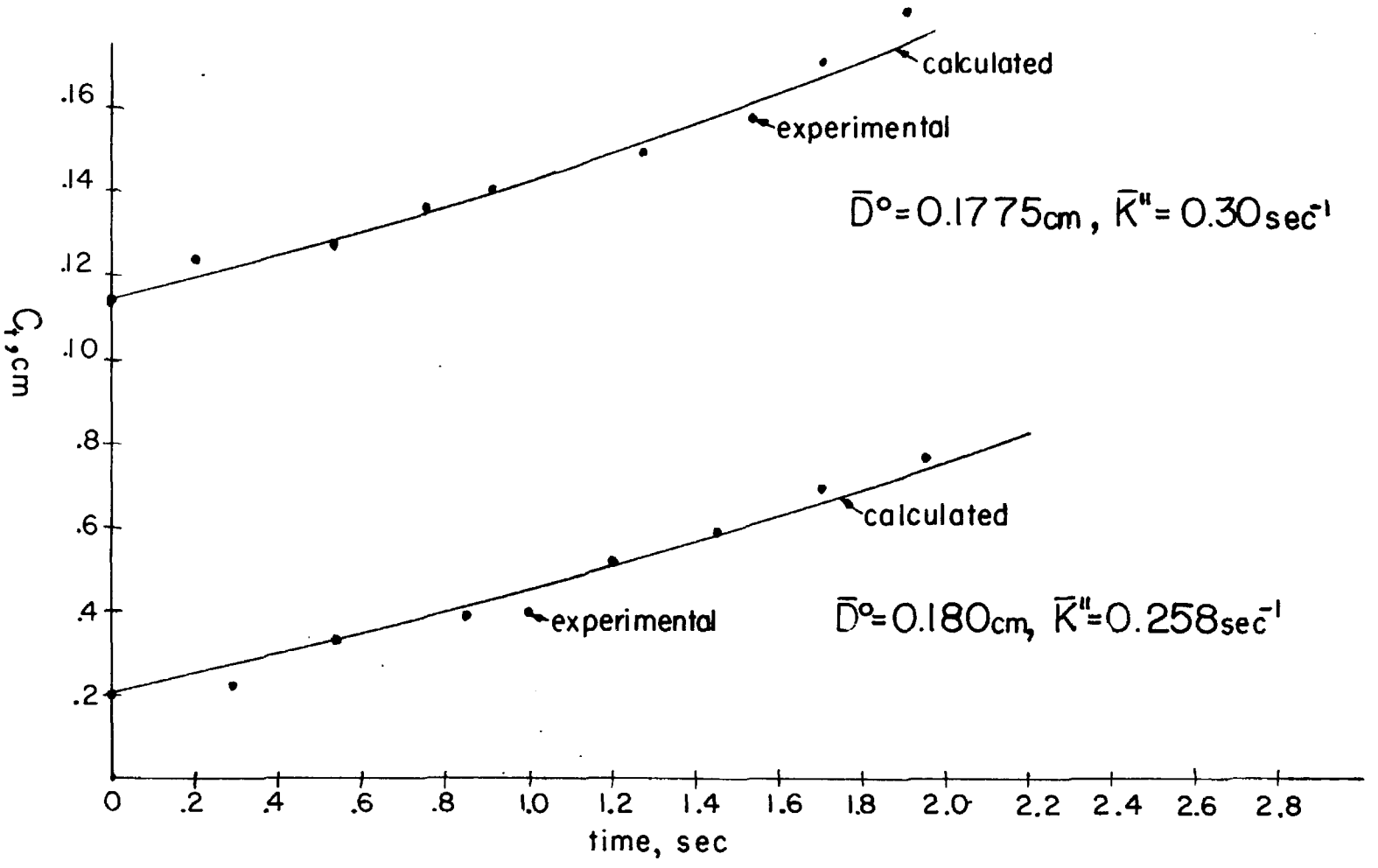

FIGURE 34. PLOT OF EXPERIMENTAL AND CALCULATED VALUES FOR C_t vs time WHERE $C_t = C^o + \bar{D}^o(1 - \sqrt{K'' t^{-1}})$